Springer

Dear Author,

Here are the proofs of your article.

- You can submit your corrections **online**, via **e-mail** or by **fax**.
- For **online** submission please insert your corrections in the online correction form. Always indicate the line number to which the correction refers.
- You can also insert your corrections in the proof PDF and **email** the annotated PDF.
- For fax submission, please ensure that your corrections are clearly legible. Use a fine black pen and write the correction in the margin, not too close to the edge of the page.
- Remember to note the **journal title**, **article number**, and **your name** when sending your response via e-mail or fax.
- **Check** the metadata sheet to make sure that the header information, especially author names and the corresponding affiliations are correctly shown.
- **Check** the questions that may have arisen during copy editing and insert your answers/ corrections.
- **Check** that the text is complete and that all figures, tables and their legends are included. Also check the accuracy of special characters, equations, and electronic supplementary material if applicable. If necessary refer to the *Edited manuscript*.
- The publication of inaccurate data such as dosages and units can have serious consequences. Please take particular care that all such details are correct.
- Please **do not** make changes that involve only matters of style. We have generally introduced forms that follow the journal's style.
  Substantial changes in content, e.g., new results, corrected values, title and authorship are not allowed without the approval of the responsible editor. In such a case, please contact the Editorial Office and return his/her consent together with the proof.
- If we do not receive your corrections **within 48 hours**, we will send you a reminder.
- Your article will be published **Online First** approximately one week after receipt of your corrected proofs. This is the **official first publication** citable with the DOI. **Further changes are, therefore, not possible.**
- The **printed version** will follow in a forthcoming issue.

Please note

After online publication, subscribers (personal/institutional) to this journal will have access to the complete article via the DOI using the URL: http://dx.doi.org/[DOI].
If you would like to know when your article has been published online, take advantage of our free alert service. For registration and further information go to: http://www.link.springer.com.

Due to the electronic nature of the procedure, the manuscript and the original figures will only be returned to you on special request. When you return your corrections, please inform us if you would like to have these documents returned.

Metadata of the article that will be visualized in OnlineFirst

Please note: Images will appear in color online but will be printed in black and white.

ArticleTitle	Gedanken experiments for the determination of two-dimensional linear second gradient elasticity coefficients	
Article Sub-Title		
Article CopyRight	Springer Basel (This will be the copyright line in the final PDF)	
Journal Name	Zeitschrift für angewandte Mathematik und Physik	
Corresponding Author	Family Name	**Placidi**
	Particle	
	Given Name	**Luca**
	Suffix	
	Division	
	Organization	International Telematic University Uninettuno
	Address	C. so Vittorio Emanuele II, 39 00186, Rome, Italy
	Email	luca.placidi@uninettunouniversity.net
Author	Family Name	**Andreaus**
	Particle	
	Given Name	**Ugo**
	Suffix	
	Division	
	Organization	Universitá di Roma La Sapienza
	Address	Rome, Italy
	Email	
Author	Family Name	**Corte**
	Particle	
	Given Name	**Alessandro Della**
	Suffix	
	Division	
	Organization	Universitá di Roma La Sapienza
	Address	Rome, Italy
	Email	
Author	Family Name	**Lekszycki**
	Particle	
	Given Name	**Tomasz**
	Suffix	
	Division	Tomasz Lekszycki, Faculty of Engineering Production,
	Organization	Warsaw University of Technology
	Address	Warsaw, Poland
	Email	

Schedule	Received	31 March 2015

	Revised	7 September 2015
	Accepted	

Abstract	In the present paper, a two-dimensional solid consisting of a linear elastic isotropic material, for which the deformation energy depends on the second gradient of the displacement, is considered. The strain energy is demonstrated to depend on 6 constitutive parameters: the 2 Lamé constants (λ and μ) and 4 more parameters (instead of 5 as it is in the 3*D*-case). Analytical solutions for classical problems such as heavy sheet, bending and flexure are provided. The idea is very simple: The solutions of the corresponding problem of first gradient classical case are imposed, and the corresponding forces, double forces and wedge forces are found out. On the basis of such solutions, a method is outlined, which is able to identify the six constitutive parameters. Ideal (or Gedanken) experiments are designed in order to write equations having as unknowns the six constants and as known terms the values of suitable experimental measurements.

Keywords (separated by '-')	Second gradient - Elasticity - Variational approach - Isotropy - Analytical solution
Footnote Information	

Journal: 33
Article: 588

Author Query Form

Please ensure you fill out your response to the queries raised below and return this form along with your corrections

Dear Author

During the process of typesetting your article, the following queries have arisen. Please check your typeset proof carefully against the queries listed below and mark the necessary changes either directly on the proof/online grid or in the 'Author's response' area provided below

Query	Details required	Author's response
1.	Please confirm the inserted city names 'Rome, Warsaw' are correct and amend if necessary.	I confirm
2.	Please provide MSC codes. For more details, if required, kindly visit http://www.ams.org/msc/.	74B99, 74Q15
3.	Please check the abbreviated journal titles in the references [17, 25, 32, 33, 42, 45, 56, 57, 67].	I confirm
4.	Please update Ref. [55] with year, volume number and page range.	We still do not have a doi for the reference [55], that therefore can not be updated

Besides, consider the following corrections:
Page 5, line 9, erase "out"
Page 6, line 41, insert "defined and"
Page 6, line 50, insert ". First, we define the following problems"
Page 6, line 71, insert space
Page 6, line 77, insert space
Page 7, line 95, insert space
Page 8, line 111, remove one of the two "+" from the equation
Page 9, line 145, erase "following"
Page 12, line 247, insert space
Page 17, line 330, insert space
Page 29, reference 13, please, update as indicated
Page 30, reference 31, update as indicated
Page 30, reference 42, update as indicated

Z. Angew. Math. Phys.

DOI 10.1007/s00033-015-0588-9

Zeitschrift für angewandte Mathematik und Physik ZAMP

Gedanken experiments for the determination of two-dimensional linear second gradient elasticity coefficients

Luca Placidi, Ugo Andreaus, Alessandro Della Corte and Tomasz Lekszycki

Abstract. In the present paper, a two-dimensional solid consisting of a linear elastic isotropic material, for which the deformation energy depends on the second gradient of the displacement, is considered. The strain energy is demonstrated to depend on 6 constitutive parameters: the 2 Lamé constants (λ and μ) and 4 more parameters (instead of 5 as it is in the $3D$-case). Analytical solutions for classical problems such as heavy sheet, bending and flexure are provided. The idea is very simple: The solutions of the corresponding problem of first gradient classical case are imposed, and the corresponding forces, double forces and wedge forces are found ~~out~~. On the basis of such solutions, a method is outlined, which is able to identify the six constitutive parameters. Ideal (or Gedanken) experiments are designed in order to write equations having as unknowns the six constants and as known terms the values of suitable experimental measurements.

Keywords. Second gradient · Elasticity · Variational approach · Isotropy · Analytical solution.

1. Introduction

It has been known since the first half of the nineteenth century, namely since the pioneering works by Gabrio Piola [13], that many microstructural effects in mechanical systems can be modeled by means of continuum theories [23]. A natural way to build a suitable theoretical model, when strongly localized deformation features are observed [2,35,53,54,58], is to complement the displacement field with some additional kinematical descriptors [11,34,36,42,46,52,67]; this approach leads to the so-called micromorphic models. Another possibility is to consider higher-order gradient theories, in which the deformation energy depends on second and/or higher gradients of the displacement [17,33,40]. This is done in the literature for both monophasic systems (see [14,15,19,22,24,25,44,57], in which continuous systems are investigated, and [1,26,56,64] for cases of lattice/woven structures) and for biphasic (see, e.g., [16,18,20,21,41,45,60,61]) or granular materials [72]. Unlike classical Cauchy continua [4,62,63], second- and higher-order continua can respond to concentrated forces and other generalized contact actions (highly localized stress/strain concentration effects are studied, e.g., in [10]). This theoretical feature is becoming increasingly important for practical and applicative reasons in the last years, as the novelties in manufacturing procedures (due to, e.g., 3D printing and self-assembly) are making possible the realization of a much wider class of new architectured materials [12]. The investigation of the continuous limit of such materials is therefore of great importance for both theoretical and technological reasons. In [3], the simplest model of strain gradient elasticity is considered. It appears that many possible sets of moduli can be defined, each of them constituted of 4 moduli—a result that is confirmed in the present work. The deficiencies of classical approaches when the material behavior exhibits size-scale effects are investigated in [59], and in [47] a novel invariance requirement (micro-randomness) in addition to isotropy is formulated, which implies conformal invariance of the curvature. The numerical investigation of structures of the type considered also requires special attention, and it is therefore important in the development of novel techniques [5–9,37,38,48–51,65] or the proper employment of the existing ones (see, for instance, [68], where Galerkin boundary element method is used to address a class of strain gradient elastic materials).

. First, we define the following problems

defined and

A two-dimensional solid consisting of a linear elastic isotropic material is considered in this paper. The strain energy is expressed as a function of the strain and its gradient. The balance equations and the boundary conditions are found using the variational method, setting equal to zero the first variation of the total potential energy. Thus, forces, double forces and wedge forces are highlighted, the existence of which is necessary for the satisfaction of the above balance equations. Adopting the general constitutive relation proposed by Midlin for second gradient $3D$ solids and specializing it to the $2D$ case, the strain energy is demonstrated to depend on 6 constitutive parameters: the 2 Lamé constants (λ and μ) and other 4 (instead of 5 for the $3D$ case) constants (A, B, C and D). Analytical solutions of the same problem can be found in [55], see also [66]. However, in this paper a method is outlined, which is able to identify the six constitutive parameters (see [69] for another identification technique) and to design some ideal experiments that allow to write equations having as unknowns the six constants and as known terms the values of the experimental measurements of appropriately selected quantities. The ideal experiments are as simple as possible: heavy sheet, bending and flexure. In each of the three problems, the solution of the corresponding classical (first gradient) solution is imposed, and the resulting forces, double forces and wedge forces are found out. At this point, the variables to be measured experimentally are chosen in order to identify the six unknown parameters. The heavy sheet experiment (rectangular sample) provides two conditions on λ and μ and one condition on D; the trapezoidal sample, in turn, provides a condition on A, B and C; the bending provides 1 condition combining the whole set of six coefficients λ, μ A, B, C and D; Finally, the flexure provides 4 conditions on the whole set of six coefficients λ, μ A, B, C and D for a total of 9 conditions. The six constants can then be identified from 84 subsets selected from the 9 equations in 6 unknowns.

Therefore, the result of this work provides a theoretical and practical guide to the design of laboratory experiments, capable of identifying the constitutive parameters of $2D$ solids characterized by a strain energy dependent on the first and second gradient of the displacement.

2. Formulation of the problem

2.1. Definition of the deformation energy functional

Please, insert a space

X_i are the coordinates of the material points of the $2D$ body $\mathcal{B}$ in the reference configuration. The internal energy density functional $U(G_{ij}, G_{ij,h})$ depends not only on the deformation matrix $G_{ij} = (F_{hi}F_{hj} - \delta_{ij})/2$ but also on its gradient $G_{ij,h}$, where $F_{ij} = \chi_{i,j}, \chi_i$ is the placement function and subscript j after comma indicates derivative with respect to X_j. The energy functional $\mathcal{E}(u_i(X_i))$ is given by the contributions of the internal and the external energies as follows,

$$\mathcal{E}(u_i(X_i)) = \iint\limits_{\mathcal{B}} \left[U(G_{ij}, G_{ij,h}) - b_\alpha^{\text{ext}} u_\alpha\right] - \oint\limits_{\partial\mathcal{B}} \left[t_\alpha^{\text{ext}} u_\alpha + \tau_\alpha^{\text{ext}} u_{\alpha,j} n_j\right] - \int\limits_{[\partial\partial\mathcal{B}]} f_\alpha^{\text{ext}} u_\alpha \tag{1}$$

where u_i is the ith component of the displacement field and $b_\alpha^{\text{ext}}, t_\alpha^{\text{ext}}, \tau_\alpha^{\text{ext}}$ and f_α^{ext} are the external actions: b_α^{ext} is the external force per unit area and is applied on the whole two-dimensional domain$\mathcal{B}$; t_α^{ext} and τ_α^{ext} are the external force and double force (respectively) and are applied on the one-dimensional boundary $\partial\mathcal{B}$ of the domain $\mathcal{B}$; and f_α^{ext} is the external concentrated force applied on the set of points belonging to the boundary of the boundary $[\partial\partial\mathcal{B}]$, so that the last integral has to be intended as relative to a discrete measure concentrated on the vertexes and can also be represented as the sum of the external works made by the concentrated forces acting on each vertices of the domain. In other words, if we define the boundary $\partial\mathcal{B}$ as the union of m regular partsΣ_c with $c = 1, \ldots, m$ and $[\partial\partial\mathcal{B}]$ as the union of the corresponding m vertex points $\mathcal{V}_c$ with $c = 1, \ldots, m$,

$$\partial\mathcal{B} = \bigcup_{c=1}^{m} \Sigma_c, \qquad [\partial\partial\mathcal{B}] = \bigcup_{c=1}^{m} \mathcal{V}_c,$$

then the line and vertex integrals of a generic field $g(X_i)$ are represented as follows,

$$\oint_{\partial\mathcal{B}} g(X_i) = \sum_{c=1}^{m} \int_{\Sigma_c} g(X_i), \qquad \int_{[\partial\partial\mathcal{B}]} g(X_i) = \sum_{c=1}^{m} g(X_i^c) \tag{2}$$

where X_i^c are the coordinates of the vertex $\mathcal{V}_c$.

2.2. Formulation of the variational principle

If we assume $\delta\mathcal{E} = 0$, then from (1) we get the final form of the system of partial differential equations, which can be explicited once kinematical restrictions are defined. The procedure to find the minimum of a deformation energy functional $\mathcal{E}$ is standard, see [55]. The result is given by reporting the variation of the deformation energy functional,

Please, insert a space

$$\begin{aligned} \delta\mathcal{E} = &- \iint_{\mathcal{B}} \delta u_\alpha \left[\left(F_{\alpha i} \left(S_{ij} - P_{ijh} \right) \right)_{,j} + b_\alpha^{\text{ext}} \right] \\ &+ \oint_{\partial\mathcal{B}} \left[\delta u_\alpha \left(t_\alpha - t_\alpha^{\text{ext}} \right) + \delta u_{\alpha,j} n_j \left(\tau_\alpha - \tau_\alpha^{\text{ext}} \right) \right] \\ &+ \int_{\partial\partial\mathcal{B}} \delta u_\alpha f_\alpha - \int_{[\partial\partial\mathcal{B}]} \delta u_\alpha f_\alpha^{\text{ext}}, \end{aligned} \tag{3}$$

where the so-called contact force t_α, contact double force τ_α and contact wedge force f_α are defined,

$$t_\alpha = F_{\alpha i} \left(S_{ij} - P_{ijh,h} \right) n_j - P_{ka} \left(F_{\alpha i} P_{ihj} P_{ah} n_j \right)_{,k} \tag{4}$$

$$\tau_\alpha = F_{\alpha i} P_{ijk} n_j n_k \tag{5}$$

$$f_\alpha = F_{\alpha i} \nu_k P_{kh} P_{ihj} n_j \tag{6}$$

and n_i is the normal to the boundary$\partial\mathcal{B}$, P_{ij} is its tangential projector operator ($P_{ij} = \delta_{ij} - n_i n_j$), ν_k is the external tangent unit vector defined on the side of the wedge it is considered, and stress and hyper stress are defined,

$$S_{ij} = \frac{\partial U}{\partial G_{ij}}, \qquad P_{ijh} = \frac{\partial U}{\partial G_{ij,h}}. \tag{7}$$

The integral

$$\int_{\partial\partial\mathcal{B}} \delta u_\alpha f_\alpha = \int_{\partial\partial\mathcal{B}} \delta u_\alpha F_{\alpha i} \nu_k P_{kh} P_{ihj} n_j$$

is intended as the sum of the integrand for each vertex, and for every vertex we intend the sum of the contribution of the two sides corresponding to that vertex, i.e.,

$$\int_{\partial\partial\mathcal{B}} \delta u_\alpha F_{\alpha i} \nu_k P_{kh} P_{ihj} n_j = \sum_{c=1}^{m} \left(\delta u_\alpha^c F_{\alpha i}^c \nu_k^{cl} P_{kh}^{cl} P_{ihj}^c n_j^{cl} + \delta u_\alpha^c F_{\alpha i}^c \nu_k^{cr} P_{kh}^{cr} P_{ihj}^c n_j^{cr} \right),$$

where the superscript c of a generic variable g means the value $g(X_i^c)$ of such variable at the vertex $\mathcal{V}_c$, the superscript cl of a generic variable g means the value $g(X_i^c)$ of such variable at the vertex $\mathcal{V}_c$ relative to the left-hand side and the superscript cr of a generic variable g means the value $g(X_i^c)$ of such variable at the vertex $\mathcal{V}_c$ relative to the right-hand side.

Journal: 33 Article No.: 588 TYPESET DISK LE CP Disp.:2015/9/22 Pages: 27

2.3. The deformation energy functional for 2D linear second gradient elasticity

In Mindlin [43], a general form of the density of the deformation energy functional of a linear isotropic second gradient elastic material is given,

Please, remove one of the two "+"

$$U\left(G_{ij},G_{ij,h}\right)=\frac{\lambda}{2}G_{ii}G_{jj}+\mu G_{ij}G_{ij}++4\alpha_1 G_{aa,b}G_{bc,c}+\alpha_2 G_{aa,b}G_{cc,b}+4\alpha_3 G_{ab,a}G_{cb,c}$$
$$+2\alpha_4 G_{ab,c}G_{ab,c}+4\alpha_5 G_{ab,c}G_{ac,b} \tag{8}$$

where λ and μ are the Lamé's coefficients and α_i with $i=1,2,3,4,5$ are the 5 second gradient constitutive parameters. Although the bulk modulus κ and the shear modulus μ are usually the most convenient pair of elastic constants for the description of the elastic properties of an isotropic material (on isotropy-related properties of classical, first gradient, linear elastic materials, see, e.g., [27–32,39,70,71]), for our expression of deformation energy density (8), we prefer to employ the Lamé's coefficients λ and μ.

In the same reference [43], in order to have the positive definiteness of U, the following constraints on the 7 constitutive parameters must be satisfied,

$$\begin{gathered}\mu>0,\quad 3\lambda+2\mu>0,\quad -4\alpha_1+2\alpha_2+2\alpha_3+6\alpha_4-6\alpha_5>0,\quad \alpha_4>\alpha_5,\quad \alpha_4+2\alpha_5>0\\ 4\alpha_1+\alpha_2+4\alpha_3+2\alpha_4+4\alpha_5>0,\quad \alpha_1+\alpha_2<\alpha_3,\quad 4\alpha_1-2\alpha_2-2\alpha_3-3\alpha_4+3\alpha_5>0.\end{gathered} \tag{9}$$

With (8), the system of partial differential equations that can be extrapolated by the first line of (3) is calculated for the present linear case,

$$\begin{aligned}&u_{1,11}\left(\lambda+2\mu\right)+u_{1,22}\mu+u_{2,12}\left(\lambda+\mu\right)\\&\quad=u_{1,1111}B+u_{1,2222}A+u_{1,1122}\left(A+B\right)+\left(u_{2,1222}+u_{2,1112}\right)\left(B-A\right)-b_1^{\text{ext}}\end{aligned} \tag{10}$$

$$\begin{aligned}&u_{2,22}\left(\lambda+2\mu\right)+u_{2,11}\mu+u_{1,12}\left(\lambda+\mu\right)\\&\quad=u_{2,2222}B+u_{2,1111}A+u_{2,1122}\left(A+B\right)+\left(u_{1,1222}+u_{1,1112}\right)\left(B-A\right)-b_2^{\text{ext}},\end{aligned} \tag{11}$$

where

$$A=2\alpha_3+2\alpha_4+2\alpha_5,\qquad B=8\alpha_1+2\alpha_2+8\alpha_3+4\alpha_4+8\alpha_5. \tag{12}$$

The definitions of the strain matrix $G_{ij}=\left(F_{hi}F_{hj}-\delta_{ij}\right)/2$ and its gradient $G_{ij,h}$ allow us to write the deformation energy density U as a function $\tilde{U}$ only of the displacement fields u_1 and u_2 in the two-dimensional case,

$$\begin{aligned}U\left(G_{ij},G_{ij,h}\right)=\tilde{U}\left(u_i\right)&=\left(\lambda+2\mu\right)\left(u_{1,1}^2+u_{2,2}^2\right)+\mu\left(u_{1,2}^2+u_{2,1}^2\right)+2\lambda u_{1,1}u_{2,2}+2\mu u_{1,2}u_{2,1}\\&+\frac{1}{2}A\left(u_{1,22}^2+u_{2,11}^2\right)+\frac{1}{2}B\left(u_{1,11}^2+u_{2,22}^2\right)+C\left(u_{1,12}^2+u_{2,12}^2\right)\\&+2D\left(u_{1,11}u_{2,12}+u_{2,22}u_{1,12}\right)\\&+\frac{1}{2}\left(A+B-2C\right)\left(u_{1,11}u_{1,22}+u_{2,11}u_{2,22}\right)\\&+\left(B-A-2D\right)\left(u_{1,12}u_{2,11}+u_{1,22}u_{2,12}\right),\end{aligned} \tag{13}$$

where

$$C=2\alpha_1+\alpha_2+\alpha_3+3\alpha_4+5\alpha_5,\qquad D=3\alpha_1+\alpha_2+2\alpha_3. \tag{14}$$

Thus, the 5 independent coefficients of an isotropic three-dimensional second gradient elastic material reduce to 4 in the two-dimensional case. In terms of the new set (λ,μ,A,B,C and D) of constitutive coefficients, the positive definiteness of the deformation energy functional (13) is guaranteed by the classical (first gradient) two-dimensional restrictions:

$$\mu>0,\quad \lambda+\mu>0,$$

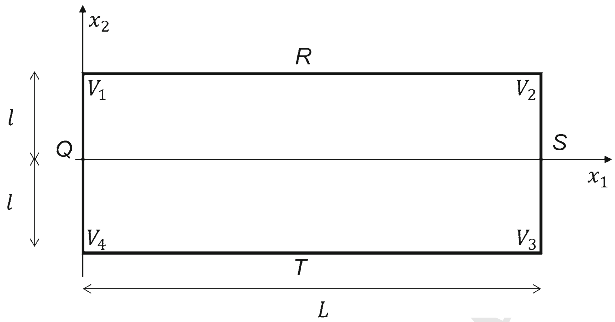

FIG. 1. Picture of the two-dimensional body $\mathcal{B}$

and by the positive definiteness of the ~~following~~ matrix

$$\begin{pmatrix} A & 0 & \frac{1}{2}(A+B-2C) & 0 & 0 & B-A-2D \\ 0 & A & 0 & \frac{1}{2}(A+B-2C) & B-A-2D & 0 \\ \frac{1}{2}(A+B-2C) & 0 & B & 0 & 0 & 2D \\ 0 & \frac{1}{2}(A+B-2C) & 0 & B & 2D & 0 \\ 0 & B-A-2D & 0 & 2D & 2C & 0 \\ B-A-2D & 0 & 2D & 0 & 0 & 2C \end{pmatrix}.$$

Common numerical data for the graphical representations that will be given in this paper are here shown (see Fig. 1)

$$L = 2\,\mathrm{m},\ l = 1\,\mathrm{m},\ \mu = 10\,\mathrm{MPa\,m},\ \lambda = 15\,\mathrm{MPa\,m},\ \rho = 10^5\,\mathrm{kg/m^2}\ E = \frac{\mu\,(3\lambda + 2\mu)}{\lambda + \mu} = 26\,\mathrm{MPa\,m}, \tag{15}$$

$$\alpha_1 = El_m^2, \quad \alpha_2 = El_m^2, \quad \alpha_3 = 2El_m^2, \quad \alpha_4 = El_m^2, \quad \alpha_5 = \frac{1}{2}El_m^2, \quad l_m = 10\,\mathrm{cm}, \tag{16}$$

and therefore

$$A = 7El_m^2, \qquad B = 34El_m^2, \qquad C = \frac{21}{2}El_m^2, \qquad D = 8El_m^2.$$

With these data, the positive definiteness of the deformation energy functional is verified.

2.4. Balance of forces and moments

Partial differential equations (10) and (11) that govern the deformation process have been derived assuming the arbitrariness of the displacement variation δu_α inside the body. The balance of force and moments, in the present formulation, is obtained by considering the subset of admissible motions constituted by the particular case of rigid motion, which in our case is a superposition of a rigid translation u_α^0 and a rotation, e.g., around the origin and of an arbitrary angle θ,

$$u_\alpha = u_\alpha^0 + \theta \varepsilon_{\alpha ij}\delta_{3i}X_j = u_\alpha^0 - \theta\delta_{1\alpha}X_2 + \theta\delta_{2\alpha}X_1, \Rightarrow\ \delta u_\alpha = \delta u_\alpha^0 - \delta\theta\left(\delta_{1\alpha}X_2 - \delta_{2\alpha}X_1\right). \tag{17}$$

With this assumption, we have from (13) that $U = 0$, from (4), (5) and (6) $t_\alpha = 0, \tau_\alpha = 0$ and $f_\alpha = 0$, respectively, while the variation of the deformation energy functional is

$$0 = -\delta\mathcal{E} = \iint\limits_{\mathcal{B}} \delta u_\alpha b_\alpha^{\mathrm{ext}} + \oint\limits_{\partial\mathcal{B}} \left[\delta u_\alpha t_\alpha^{\mathrm{ext}} + \delta u_{\alpha,j} n_j \tau_\alpha^{\mathrm{ext}}\right] + \int\limits_{[\partial\partial\mathcal{B}]} \delta u_\alpha f_\alpha^{\mathrm{ext}}. \tag{18}$$

Inserting the right-hand side of (17) into the (18) yields

$$0 = -\delta\mathcal{E} = \delta u_\alpha^0 \left\{ \iint\limits_{\mathcal{B}} b_\alpha^{\text{ext}} + \oint\limits_{\partial\mathcal{B}} t_\alpha^{\text{ext}} + \int\limits_{[\partial\partial\mathcal{B}]} f_\alpha^{\text{ext}} \right\}$$
$$-\delta\theta \left\{ \iint\limits_{\mathcal{B}} X_2 b_1^{\text{ext}} - X_1 b_2^{\text{ext}} + \oint\limits_{\partial\mathcal{B}} \left[X_2 t_1^{\text{ext}} - X_1 t_2^{\text{ext}} + n_2 \tau_1^{\text{ext}} - n_1 \tau_2^{\text{ext}} \right] + \int\limits_{[\partial\partial\mathcal{B}]} X_2 f_1^{\text{ext}} - X_1 f_2^{\text{ext}} \right\}$$

Thus, for an arbitrary pure translation ($\delta\theta = 0$) we have the so-called balance of forces,

$$\iint\limits_{\mathcal{B}} b_\alpha^{\text{ext}} + \sum_{c=1}^{m} \int\limits_{\Sigma_c} t_\alpha^{\text{ext}} + \sum_{c=1}^{m} f_\alpha^{\text{ext}} \left(X_i^c \right) = 0, \tag{19}$$

and for an arbitrary pure rotation ($\delta u_\alpha^0 = 0$) we have the so-called balance of moments,

$$\iint\limits_{\mathcal{B}} X_2 b_1^{\text{ext}} - X_1 b_2^{\text{ext}} + \sum_{c=1}^{m} \int\limits_{\Sigma_c} \left[X_2 t_1^{\text{ext}} - X_1 t_2^{\text{ext}} + n_2 \tau_1^{\text{ext}} - n_1 \tau_2^{\text{ext}} \right] + \sum_{c=1}^{m} \left(X_2^c f_1^{\text{ext}} - X_1^c f_2^{\text{ext}} \right) = 0 \tag{20}$$

where we have used the definitions given in Eqs. (2).

3. The case of a rectangle

3.1. The general framework of straight lines

In Fig. 1, we represent the scheme of a rectangle with side names Q, R, S and T and vertex names V_1, V_2, V_3 and V_4. In this case and for small displacements, the sides are straight lines, and the contact force in (4), the contact double force in (5) and the contact wedge force (6) are

$$t_\alpha = S_{\alpha j} n_j - \left(P_{\alpha jh,h} + P_{\alpha hj,h} \right) n_j + P_{\alpha hj,k} n_h n_k n_j, \; \tau_\alpha = P_{\alpha jk} n_j n_k, \; f_\alpha = \nu_i n_j P_{i\alpha j}, \tag{21}$$

that, in terms of the displacement fields, yield,

$$\begin{aligned} t_\alpha = {} & \lambda u_{a,a} n_\alpha + \mu u_{\alpha,j} n_j + \mu u_{j,\alpha} n_j - u_{a,abb} n_\alpha \left(6\alpha_1 + 2\alpha_2 + 4\alpha_3 \right) \\ & - u_{a,\alpha\alpha k} n_k \left(6\alpha_1 + 2\alpha_2 + 4\alpha_3 + 2\alpha_4 + 8\alpha_5 \right) - u_{\alpha,aak} n_k \left(2\alpha_3 + 4\alpha_4 + 6\alpha_5 \right) \\ & - u_{k,\alpha aa} n_k \left(2\alpha_1 + 2\alpha_3 + 2\alpha_4 + 6\alpha_5 \right) + u_{a,ajk} n_\alpha n_j n_k \left(4\alpha_1 + 2\alpha_2 + 2\alpha_3 \right) \\ & + u_{j,aak} n_\alpha n_j n_k \left(2\alpha_1 + 2\alpha_3 \right) + u_{\alpha,abc} n_a n_b n_c \left(2\alpha_4 + 2\alpha_5 \right) + u_{a,\alpha bc} n_a n_b n_c \left(2\alpha_4 + 6\alpha_5 \right), \end{aligned} \tag{22}$$

$$\begin{aligned} \tau_\alpha = {} & u_{a,ab} n_\alpha n_b \left(4\alpha_1 + 2\alpha_2 + 2\alpha_3 \right) + u_{a,bb} n_\alpha n_a \left(2\alpha_1 + 2\alpha_3 \right) \\ & + \left(2\alpha_1 + 2\alpha_3 \right) u_{a,a\alpha} + u_{\alpha,ab} n_a n_b \left(2\alpha_4 + 2\alpha_5 \right) + 2\alpha_3 u_{\alpha,aa} + u_{a,\alpha b} n_a n_b \left(2\alpha_4 + 6\alpha_5 \right). \end{aligned} \tag{23}$$

We remark that the formulation expressed in (22) and (23) can also be used in the three-dimensional case. This is the reason why (22) and (23) are expressed in terms of the 5 three-dimensional constitutive coefficients α_i with $i = 1, 2, 3, 4, 5$ and not in terms of the 4 two-dimensional constitutive coefficients A, B, C and D.

Journal: 33 Article No.: 588 TYPESET DISK LE CP Disp.:2015/9/22 Pages: 27

3.2. Sides

The characterization of side S is done by setting $n_i = \delta_{i1}$. Thus, from (22) with $\alpha = 1, 2$, and from (23) with $\alpha = 1, 2$, we have

$$t_1 = t_1^S = u_{1,1}(\lambda + 2\mu) + u_{2,2}\lambda - Bu_{1,111} - 2Du_{2,222} - \frac{1}{2}(A + B + 2C)\, u_{1,122} - (B - A)\, u_{2,211}, \tag{24}$$

$$t_2 = t_2^S = \mu(u_{1,2} + u_{2,1}) - (B - A)\, u_{1,112} - (B - A - 2D)\, u_{1,222} - Au_{2,111} - \frac{1}{2}(A + B + 2C)\, u_{2,122}, \tag{25}$$

$$\tau_1 = \tau_1^S = Bu_{1,11} + \frac{1}{2}(A + B - 2C)\, u_{1,22} + 2Du_{2,12}, \tag{26}$$

$$\tau_2 = \tau_2^S = (B - A - 2D)\, u_{1,12} + Au_{2,11} + \frac{1}{2}(A + B - 2C)\, u_{2,22}. \tag{27}$$

The characterization of side Q is done by setting $n_i = -\delta_{i1}$. Thus, from (22) with $\alpha = 1, 2$, and from (23) with $\alpha = 1, 2$, we have

$$t_1 = t_1^Q = -u_{1,1}(\lambda + 2\mu) - u_{2,2}\lambda + Bu_{1,111} + 2Du_{2,222} + \frac{1}{2}(A + B + 2C)\, u_{1,122} + (B - A)\, u_{2,211}, \tag{28}$$

$$t_2 = t_2^Q = -\mu(u_{1,2} + u_{2,1}) + (B - A)\, u_{1,112} + (B - A - 2D)\, u_{1,222} + Au_{2,111} + \frac{1}{2}(A + B + 2C)\, u_{2,122}, \tag{29}$$

$$\tau_1 = \tau_1^Q = Bu_{1,11} + \frac{1}{2}(A + B - 2C)\, u_{1,22} + 2Du_{2,12}, \tag{30}$$

$$\tau_2 = \tau_2^Q = (B - A - 2D)\, u_{1,12} + Au_{2,11} + \frac{1}{2}(A + B - 2C)\, u_{2,22}. \tag{31}$$

We remark that t_1^Q in (28) and t_2^Q in (29) are the opposite of t_1^S in (24) and of t_2^S in (25), respectively, and that τ_1^Q in (30) and τ_2^Q in (31) are the same of τ_1^S in (26) and of τ_2^S in (27), respectively.

The characterization of side R is done by setting $n_i = \delta_{i2}$. Thus, from (22) with $\alpha = 1, 2$, and from (23) with $\alpha = 1, 2$, we have

$$t_1 = t_1^R = \mu(u_{1,2} + u_{2,1}) - (B - A)\, u_{2,122} - (B - A - 2D)\, u_{2,111} - Au_{1,222} - \frac{1}{2}(A + B + 2C)\, u_{1,112}, \tag{32}$$

$$t_2 = t_2^R = u_{2,2}(\lambda + 2\mu) + u_{1,1}\lambda - Bu_{2,222} - 2Du_{1,111} - \frac{1}{2}(A + B + 2C)\, u_{2,112} - (B - A)\, u_{1,122}, \tag{33}$$

$$\tau_1 = \tau_1^R = (B - A - 2D)\, u_{2,12} + Au_{1,22} + \frac{1}{2}(A + B - 2C)\, u_{1,11}, \tag{34}$$

$$\tau_2 = \tau_2^R = Bu_{2,22} + \frac{1}{2}(A + B - 2C)\, u_{2,11} + 2\mathrm{D}u_{1,12}. \tag{35}$$

We remark that, because of isotropy, t_1^R in (32) and t_2^R in (33) are the same of t_2^S in (25) and of t_1^S in (24), respectively, by changing the indexes 1 and 2. Similarly, because of isotropy, τ_1^R in (34) and τ_2^R in (35) are the same of τ_2^S in (26) and of τ_1^S in (27), respectively, by changing the indexes 1 and 2.

Journal: 33 Article No.: 588 ☐ TYPESET ☐ DISK ☐ LE ☐ CP Disp.:2015/9/22 Pages: 27

Finally, the characterization of side T is done by setting $n_i = -\delta_{i2}$. Thus, from (22) with $\alpha = 1, 2$ and from (23) with $\alpha = 1, 2$, we have

$$t_1 = t_1^T = -\mu\left(u_{1,2} + u_{2,1}\right) + \left(B - A\right) u_{2,122} + \left(B - A - 2D\right) u_{2,111} + A u_{1,222} + \frac{1}{2}\left(A + B + 2C\right) u_{1,112}, \tag{36}$$

$$t_2 = t_2^T = -u_{2,2}\left(\lambda + 2\mu\right) - u_{1,1}\lambda + B u_{2,222} + 2D u_{1,111} + \frac{1}{2}\left(A + B + 2C\right) u_{2,112} + \left(B - A\right) u_{1,122}, \tag{37}$$

$$\tau_1 = \tau_1^T = \left(B - A - 2D\right) u_{2,12} + A u_{1,22} + \frac{1}{2}\left(A + B - 2C\right) u_{1,11}, \tag{38}$$

$$\tau_2 = \tau_2^T = B u_{2,22} + \frac{1}{2}\left(A + B - 2C\right) u_{2,11} + 2\mathrm{D} u_{1,12}. \tag{39}$$

We remark that t_1^T in (36) and t_2^T in (37) are the opposite of t_1^R in (32) and of t_2^R in (33), respectively, and that τ_1^T in (38) and τ_2^T in (39) are the same of τ_1^R in (34) and of τ_2^R in (35), respectively.

3.3. Vertices

The last term of (3) is reduced, because of $(2)_2$, to

$$\begin{aligned}
&\int\limits_{\partial\partial\mathcal{B}} \delta u_\alpha f_\alpha - \int\limits_{[\partial\partial\mathcal{B}]} \delta u_\alpha f_\alpha^{\text{ext}} \\
&\quad = \left[\delta u_\alpha\left(f_\alpha\left(Q\right) + f_\alpha\left(R\right) - f_\alpha^{\text{ext}}\right)\right]_{V_1} + \left[\delta u_\alpha\left(f_\alpha\left(R\right) + f_\alpha\left(S\right) - f_\alpha^{\text{ext}}\right)\right]_{V_2} \\
&\qquad + \left[\delta u_\alpha\left(f_\alpha\left(S\right) + f_\alpha\left(T\right) - f_\alpha^{\text{ext}}\right)\right]_{V_3} + \left[\delta u_\alpha\left(f_\alpha\left(T\right) + f_\alpha\left(Q\right) - f_\alpha^{\text{ext}}\right)\right]_{V_4},
\end{aligned} \tag{40}$$

where $\left[f\left(\partial_i\mathcal{B}\right)\right]_{\mathcal{V}_j}$ is the contact wedge force calculated for the wedge $\mathcal{V}_j$ and for the boundary $\partial_i\mathcal{B}$. We have already pointed out the form of the unit normals for each side. The form of the tangent ν_i is set taking into account that such tangent points off the edge. Thus,

$$\begin{array}{llllll}
\partial_i\mathcal{B} = Q, & \mathcal{V}_j = V_1 & \Longrightarrow & n_j = -\delta_{1j} & \nu_i = \delta_{i2}, & \Longrightarrow \quad \left[f_\alpha\left(Q\right)\right]_{V_1} = -P_{2\alpha 1} \\
\partial_i\mathcal{B} = R, & \mathcal{V}_j = V_1 & \Longrightarrow & n_j = \delta_{2j} & \nu_i = -\delta_{i1}, & \Longrightarrow \quad \left[f_\alpha\left(R\right)\right]_{V_1} = -P_{1\alpha 2} \\
\partial_i\mathcal{B} = R, & \mathcal{V}_j = V_2 & \Longrightarrow & n_j = \delta_{2j} & \nu_i = \delta_{i1}, & \Longrightarrow \quad \left[f_\alpha\left(R\right)\right]_{V_2} = P_{1\alpha 2} \\
\partial_i\mathcal{B} = S, & \mathcal{V}_j = V_2 & \Longrightarrow & n_j = \delta_{1j} & \nu_i = \delta_{i2}, & \Longrightarrow \quad \left[f_\alpha\left(S\right)\right]_{V_2} = P_{2\alpha 1} \\
\partial_i\mathcal{B} = S, & \mathcal{V}_j = V_3 & \Longrightarrow & n_j = \delta_{1j} & \nu_i = -\delta_{i2}, & \Longrightarrow \quad \left[f_\alpha\left(S\right)\right]_{V_3} = -P_{2\alpha 1} \\
\partial_i\mathcal{B} = T, & \mathcal{V}_j = V_3 & \Longrightarrow & n_j = -\delta_{2j} & \nu_i = \delta_{i1}, & \Longrightarrow \quad \left[f_\alpha\left(T\right)\right]_{V_3} = -P_{1\alpha 2} \\
\partial_i\mathcal{B} = T, & \mathcal{V}_j = V_4 & \Longrightarrow & n_j = -\delta_{2j} & \nu_i = -\delta_{i1}, & \Longrightarrow \quad \left[f_\alpha\left(T\right)\right]_{V_4} = P_{1\alpha 2} \\
\partial_i\mathcal{B} = Q, & \mathcal{V}_j = V_4 & \Longrightarrow & n_j = -\delta_{1j} & \nu_i = -\delta_{i2}, & \Longrightarrow \quad \left[f_\alpha\left(Q\right)\right]_{V_4} = P_{2\alpha 1}.
\end{array}$$

Keeping this in mind, we have that

$$\begin{aligned}
\int\limits_{\partial\partial\mathcal{B}} \delta u_\alpha\left(f_\alpha - f_\alpha^{\text{ext}}\right) = &\left[\delta u_\alpha\left(-P_{2\alpha 1} - P_{1\alpha 2} - f_\alpha^{\text{ext}}\right)\right]_{V_1} \\
&+ \left[\delta u_\alpha\left(P_{2\alpha 1} + P_{1\alpha 2} - f_\alpha^{\text{ext}}\right)\right]_{V_2} \\
&+ \left[\delta u_\alpha\left(-P_{2\alpha 1} - P_{1\alpha 2} - f_\alpha^{\text{ext}}\right)\right]_{V_3} \\
&+ \left[\delta u_\alpha\left(P_{2\alpha 1} + P_{1\alpha 2} - f_\alpha^{\text{ext}}\right)\right]_{V_4},
\end{aligned} \tag{41}$$

Please, insert a space

where$P_{2\alpha 1} + P_{1\alpha 2}$, in terms of the displacement field, becomes for $\alpha = 1$

$$P_{211} + P_{112} = 2C u_{1,12} + \left(B - A - 2D\right) u_{2,11} + 2D u_{2,22}, \tag{42}$$

Journal: 33 Article No.: 588 TYPESET DISK LE CP Disp.:2015/9/22 Pages: 27

and for $\alpha = 2$,

$$P_{221} + P_{122} = 2Cu_{2,12} + (B - A - 2D)\, u_{1,22} + 2Du_{1,11}. \tag{43}$$

3.4. Explicit form of the balances of forces and moments

The balance of force is obtained from (19)

$$\sum_{J=1,2,3,4} \left[f_\alpha^{\text{ext}}\right]_{V_J} + \sum_{J=Q,S} \int_{-l}^{l} t_\alpha^{\text{ext},J} + \sum_{J=R,T} \int_{0}^{L} t_\alpha^{\text{ext},J} = 0.$$

The balance of moments is obtained from (20) and must be satisfied by taking into account not only the edge and wedge forces but also the double forces,

$$\begin{aligned} & l\left[f_1^{\text{ext}}\right]_{V_1} + l\left[f_1^{\text{ext}}\right]_{V_2} - L\left[f_2^{\text{ext}}\right]_{V_2} - l\left[f_1^{\text{ext}}\right]_{V_3} - L\left[f_2^{\text{ext}}\right]_{V_3} - l\left[f_1^{\text{ext}}\right]_{V_4} \\ & \quad + \int_{-l}^{l} X_2 t_1^{\text{ext},Q} + l\int_{0}^{L} t_1^{\text{ext},R} - \int_{0}^{L} X_1 t_2^{\text{ext},R} + \int_{-l}^{l} X_2 t_1^{\text{ext},S} - L\int_{-l}^{l} t_2^{\text{ext},S} - l\int_{0}^{L} t_1^{\text{ext},T} \\ & \quad - \int_{0}^{L} X_1 t_2^{\text{ext},T} + \int_{-l}^{l} \tau_2^{\text{ext},Q} + \int_{0}^{L} \tau_1^{\text{ext},R} - \int_{-l}^{l} \tau_2^{\text{ext},S} - \int_{0}^{L} \tau_1^{\text{ext},T} = 0. \end{aligned}$$

3.5. An analytical solution for the heavy sheet

3.5.1. Preliminary remarks and kinematical constraints. We consider a heavy sheet hanging by the top side R. The kinematical constraints on the displacement field are conceived in order to avoid the Poisson effect, see also the sliding system in Fig. 4. Therefore, such kinematical constraints are imposed not only on the side R but also on the two vertical sides Q and S,

$$(\delta u_2)_R = 0, \quad (\delta u_1)_Q = 0, \quad (\delta u_1)_S = 0. \tag{44}$$

In the following, we consider the general solution of this simple problem in the first gradient case. Thus, we calculate the whole set of boundary conditions to be applied in the second gradient case.

3.5.2. The external surface forces. Let us take into account the following displacement field,

$$u_1 = 0, \qquad u_2 = \frac{\rho g\,(X_2 - l)\,(3l + X_2)}{2\,(\lambda + 2\mu)}, \tag{45}$$

also represented in the first row of Fig. 2 and in the first two rows of Fig. 3. The two partial differential equations (10) and (11) are satisfied with the following external force per unit area,

$$b_1^{\text{ext}} = 0, \qquad b_2^{\text{ext}} = -\rho g, \tag{46}$$

that is the external force due to the weight where we have used the following intermediate results,

$$u_{2,2} = \frac{\rho g\,(l + X_2)}{(\lambda + 2\mu)}, \qquad u_{2,22} = \frac{\rho g}{(\lambda + 2\mu)}. \tag{47}$$

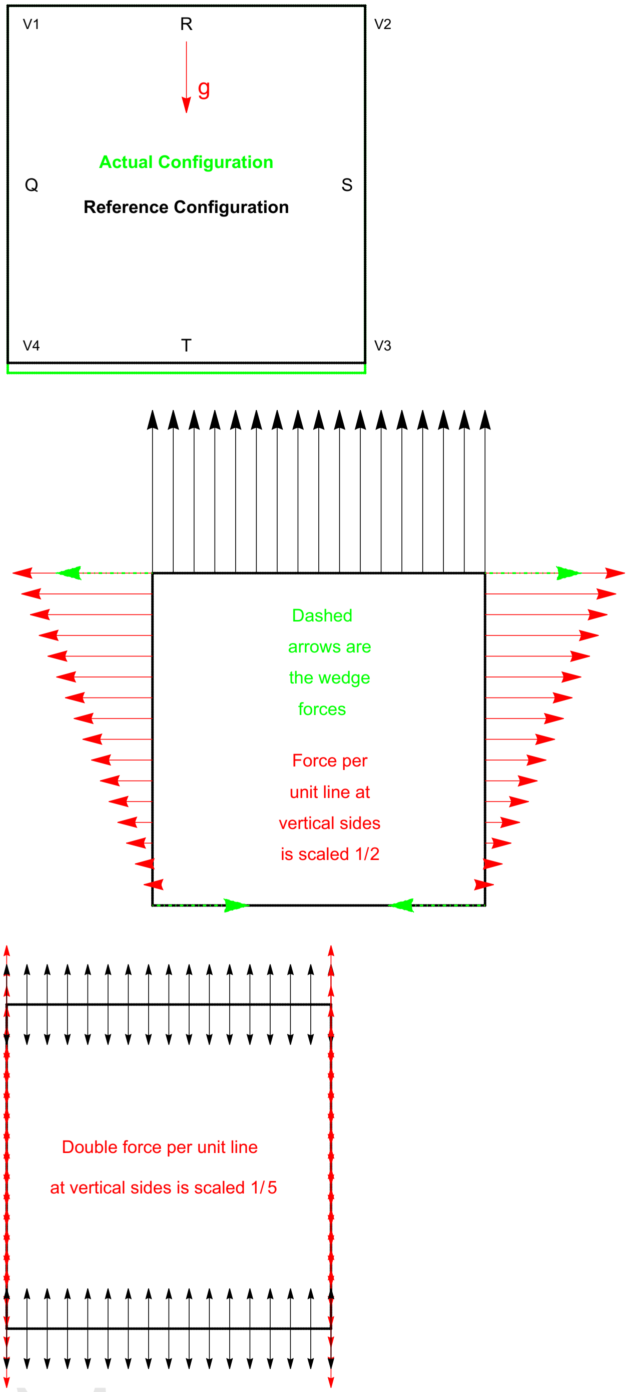

FIG. 2. A *column of figures* is represented for the heavy sheet case. In the *first row*, reference and actual configuration are represented. In the *second row*, wedge forces and force per unit *line* are represented. In the *third row*, we represent the double force per unit *line*

Journal: 33 Article No.: 588 TYPESET DISK LE CP Disp.:2015/9/22 Pages: 27

3.5.3. The external edge forces. In the following, we calculate the edge forces that are necessary to have the displacement field (45). Such forces per unit line are also graphically represented in the second row of Fig. 2 and in the third and fourth rows of Fig. 3.

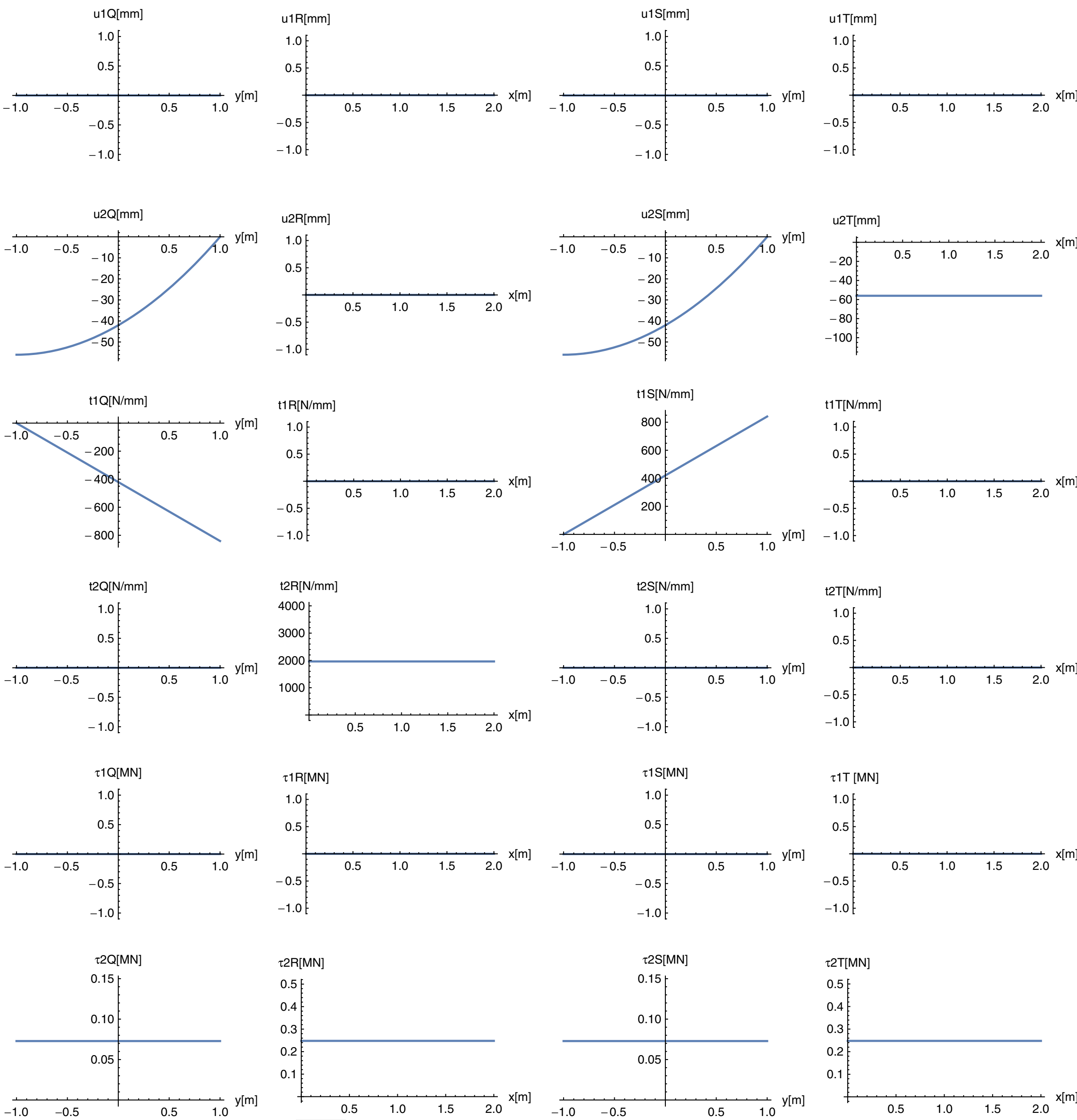

FIG. 3. A *grid of figures* represents the heavy sheet case. In the *first, second, third* and *fourth column*, we show characteristics of sides A, B, C and D, respectively. In the *first* and in the *second row*, we show the displacement fields, respectively, in the two directions. In the *third* and in the *fourth row*, we show the force per unit line fields, respectively, in the two directions. In the *fifth* and in the *sixth row*, we show the double force per unit line fields, respectively, in the two directions

Journal: 33 Article No.: 588 TYPESET DISK LE CP Disp.:2015/9/22 Pages: 27

Side S. From (24) and (45), we have

$$t_1 = t_1^{\mathrm{ext},S} = \frac{\rho g\,(l + X_2)}{(\lambda + 2\mu)}\lambda \tag{48}$$

Such force in the horizontal direction is due to the Poisson effect and it is associated with the kinematical constraint $(44)_3$. From (25), we have simply ($t_2 = t_2^{\mathrm{ext},S} = 0$), i.e., no traction condition.

Side Q. From (28) and (45), we have

$$t_1 = t_1^{\mathrm{ext},Q} = -\frac{\rho g\,(l + X_2)}{(\lambda + 2\mu)}\lambda, \tag{49}$$

that, for symmetry reasons, is the opposite of that on side S and it is connected to the kinematical constraint $(44)_2$. From (29), we have simply ($t_2 = t_2^{\mathrm{ext},Q} = 0$), i.e., no traction condition.

Side R. From (32) and (45), we have $t_1 = t_1^R = 0$ (no traction condition) in the horizontal direction and from (33) we have

$$t_2 = t_2^R = u_{2,2}\,(\lambda + 2\mu) = \frac{\rho g\,(l + X_2)}{(\lambda + 2\mu)}\,(\lambda + 2\mu) = \rho g\,(l + X_2)_{x_2 = l} = 2\rho g l, \tag{50}$$

that is the usual reaction at the upper boundary, and it is connected to the kinematical constraint $(44)_1$.

Side T. From (36) and (45), we have no traction condition ($t_1 = t_1^T = 0$) in the horizontal direction and from (37) we have

$$t_2 = t_2^T = -u_{2,2}\,(\lambda + 2\mu) = -\frac{\rho g\,(l + X_2)}{(\lambda + 2\mu)}\,(\lambda + 2\mu) = -\rho g\,(l + X_2)_{X_2 = -l} = 0, \tag{51}$$

that means that we have no reactions at the bottom of the body.

3.5.4. The external edge double forces. In the previous subsubsection, we calculated the forces per unit line that are necessary to have the solution (45) with the kinematical constraints (44). In this subsubsection, we calculate the analogous double force per unit line. Such double forces per unit line are also graphically represented in the third row of Fig. 2 and in the fifth and sixth rows of Fig. 3.

Side S. From (26) and (45), we simply have ($\tau_1 = \tau_1^{\mathrm{ext},S} = 0$) no double force condition in the horizontal direction. On the other hand, in the vertical direction from (27) and (45) we have

$$\tau_2 = \tau_2^{\mathrm{ext},S} = \frac{(A + B - 2C)\,\rho g}{2\,(\lambda + 2\mu)}. \tag{52}$$

Side Q. From (30) and (45), for symmetry reasons, we again have ($\tau_1 = \tau_1^{\mathrm{ext},Q} = 0$) no double force condition in the horizontal direction, and from (31) and (45), we have the same double force per unit line of (52),

$$\tau_2 = \tau_2^{\mathrm{ext},Q} = \frac{(A + B - 2C)\,\rho g}{2\,(\lambda + 2\mu)}. \tag{53}$$

Side R. From (34) and (45), we have ($\tau_1 = \tau_1^{\mathrm{ext},R} = 0$) no double force condition in the horizontal direction, and from (35) and (45), we have

$$\tau_2 = \tau_2^{R,ext} = \frac{\rho g B}{(\lambda + 2\mu)}. \tag{54}$$

Side T. For symmetry reasons, from (38) we have ($\tau_1 = \tau_1^{\mathrm{ext},T} = 0$) again no double force condition in the horizontal direction, and from (39) and (45), we have

$$\tau_2 = \tau_2^{T,ext} = \frac{\rho g B}{(\lambda + 2\mu)}. \tag{55}$$

3.5.5. The external wedge forces. The kinematical restrictions (44) imply no displacement at vertices V_1 and V_2 and no horizontal displacement at vertices V_3 and V_4. This means that the external (or reaction) wedge forces in order to keep the displacement field in (45) are from (41), (42) and (43),

$$f_\alpha^{\text{ext}} = -P_{2\alpha 1} - P_{1\alpha 2}$$

for wedges V_1 and V_3 and the opposite

$$f_\alpha^{\text{ext}} = P_{2\alpha 1} + P_{1\alpha 2}$$

for wedges V_2 and V_4. We have from (42), (45) and (47)

$$P_{211} + P_{112} = \frac{2D\rho g}{(\lambda + 2\mu)} \cong 0.12MN,$$

where the coefficient D is defined in (14), and the exemplifying numerical values employed are those in (15) and (16). We have from (43) and (45) and (47)

$$P_{221} + P_{122} = 0.$$

Thus, the external (or reaction) wedge forces for the 4 vertices are the following,

$$\left(f_1^{\text{ext}}\right)_{V_1} = -\frac{2D\rho g}{(\lambda + 2\mu)} \cong -0.12MN, \qquad \left(f_2^{\text{ext}}\right)_{V_1} = 0, \tag{56}$$

$$\left(f_1^{\text{ext}}\right)_{V_2} = \frac{2D\rho g}{(\lambda + 2\mu)} \cong 0.12MN, \qquad \left(f_2^{\text{ext}}\right)_{V_2} = 0, \tag{57}$$

Please insert a space

$$\left(f_1^{\text{ext}}\right)_{V_3} = -\frac{2D\rho g}{(\lambda + 2\mu)} \cong -0.12MN, \qquad \left(f_2^{\text{ext}}\right)_{V_3} = 0, \tag{58}$$

$$\left(f_1^{\text{ext}}\right)_{V_4} = \frac{2D\rho g}{(\lambda + 2\mu)} \cong 0.12MN, \qquad \left(f_2^{\text{ext}}\right)_{V_4} = 0, \tag{59}$$

that are also graphically represented in the second row of Fig. 2.

3.5.6. The trapezoidal case. Let us cut the rectangle from the vertex V_3 to a general vertex V_o in the side Q or R or at the vertex V_1, see also Fig. 4. The new side has the following normal,

$$n_j = -\sin\theta\delta_{1j} - \cos\theta\delta_{2j},$$

and, at vertexV_3, has the following tangent,

$$\nu_i = \cos\theta\delta_{1i} - \sin\theta\delta_{2i},$$

where θ is the angle between the horizontal side and the new oblique side. At the vertex V_3, the necessary external (or reaction) force must be

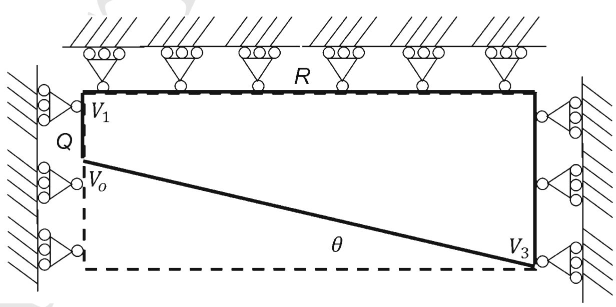

FIG. 4. Picture of the cut body$\mathcal{B}$

$$\begin{aligned}
f_{\alpha}^{\text{ext}} &= \left[f_{\alpha}(S)+f_{\alpha}(O)\right]_{V_o} = \left[\nu_i n_j P_{i\alpha j}\right]_{S,V_o} + \left[\nu_i n_j P_{i\alpha j}\right]_{O,V_o} \\
&= \left[-\delta_{2i}\delta_{1j}P_{i\alpha j}\right]_{S,V_o} - \left[\left(\cos\theta\delta_{1i}-\sin\theta\delta_{2i}\right)\left(\sin\theta\delta_{1j}+\cos\theta\delta_{2j}\right)P_{i\alpha j}\right]_{V_o} \\
&= -P_{2\alpha 1} - P_{1\alpha 1}\sin\theta\cos\theta - P_{1\alpha 2}\cos\theta\cos\theta + P_{2\alpha 1}\sin\theta\sin\theta + P_{2\alpha 2}\cos\theta\sin\theta \\
&= -\left(P_{2\alpha 1}+P_{1\alpha 2}\right)\cos^2\theta + \left(P_{2\alpha 2}-P_{1\alpha 1}\right)\sin\theta\cos\theta. \qquad (60)
\end{aligned}$$

We have for $\alpha = 1$,

$$f_1^{\text{ext}} = -\left(P_{211}+P_{112}\right)\cos^2\theta + \left(P_{212}-P_{111}\right)\sin\theta\cos\theta, \qquad (61)$$

where

$$P_{211}+P_{112} = 2Cu_{1,12} + \left(B-A-2D\right)u_{2,11} + 2Du_{2,22}, \qquad (62)$$

and

$$P_{212}-P_{111} = -\frac{1}{2}\left(B-A+2C\right)u_{1,11} - \frac{1}{2}\left(B-A-2C\right)u_{1,22} - \left(A-B+4D\right)u_{2,12}, \qquad (63)$$

while for $\alpha = 2$,

$$f_2^{\text{ext}} = -\left(P_{221}+P_{122}\right)\cos^2\theta + \left(P_{222}-P_{121}\right)\sin\theta\cos\theta, \qquad (64)$$

where

$$P_{221}+P_{122} = 2Du_{1,11} + + \left(B-A-2D\right)u_{1,22} + 2Cu_{2,12}, \qquad (65)$$

and

$$P_{222}-P_{121} = \frac{1}{2}\left(B-A-2C\right)u_{2,11} + + \frac{1}{2}\left(B-A+2C\right)u_{2,22} + \left(A-B+4D\right)u_{1,12}. \qquad (66)$$

By insertion of the solution (45) into (62), (63), (65) and (66), the forces (61) and (64) are evaluated,

$$f_1^{\text{ext}} = -\cos^2\theta\left[\frac{2\rho g D}{\left(\lambda+2\mu\right)}\right] \cong -0.12\,\cos^2\theta\,MN, \qquad (67)$$

$$f_2^{\text{ext}} = \sin\theta\cos\theta\left[\frac{\rho g}{2\left(\lambda+2\mu\right)}\left(B-A+2C\right)\right] \cong 0.17\,\sin\theta\cos\theta\,MN, \qquad (68)$$

where the exemplifying numerical values employed are those in (15) and (16).

3.6. An analytical solution for bending

Let us take into account the following displacement field,

$$\begin{aligned}
u_1 &= \frac{3M^{\text{ext}}\left(\lambda+2\mu\right)X_1X_2}{8l^3\mu\left(\lambda+\mu\right)}, \\
u_2 &= -\frac{3M^{\text{ext}}\left[\lambda X_2^2+\left(\lambda+2\mu\right)X_1^2\right]}{16l^3\mu\left(\lambda+\mu\right)}, \qquad (69)
\end{aligned}$$

also represented in the first row of Fig. 5 and in the first and second rows of Fig. 6. The two partial differential equations (10) and (11) are satisfied with null external force per unit area, $b_1^{\text{ext}} = b_2^{\text{ext}} = 0$, where we have used the following intermediate results,

$$u_{1,1} = \frac{3M^{\text{ext}}\left(\lambda+2\mu\right)X_2}{8l^3\mu\left(\lambda+\mu\right)}, \quad u_{1,12} = \frac{3M^{\text{ext}}\left(\lambda+2\mu\right)}{8l^3\mu\left(\lambda+\mu\right)}, \quad u_{1,2} = \frac{3M^{\text{ext}}\left(\lambda+2\mu\right)X_1}{8l^3\mu\left(\lambda+\mu\right)}, \qquad (70)$$

$$u_{2,1} = -\frac{3M^{\text{ext}}\left[\left(\lambda+2\mu\right)X_1\right]}{8l^3\mu\left(\lambda+\mu\right)}, \quad u_{2,11} = -\frac{3M^{\text{ext}}\left(\lambda+2\mu\right)}{8l^3\mu\left(\lambda+\mu\right)} = -u_{1,12}, \qquad (71)$$

$$u_{2,2} = -\frac{3M^{\text{ext}}\lambda X_2}{8l^3\mu\left(\lambda+\mu\right)}, \quad u_{2,22} = -\frac{3M^{\text{ext}}\lambda}{8l^3\mu\left(\lambda+\mu\right)}. \qquad (72)$$

Journal: 33 Article No.: 588 TYPESET DISK LE CP Disp.:2015/9/22 Pages: 27

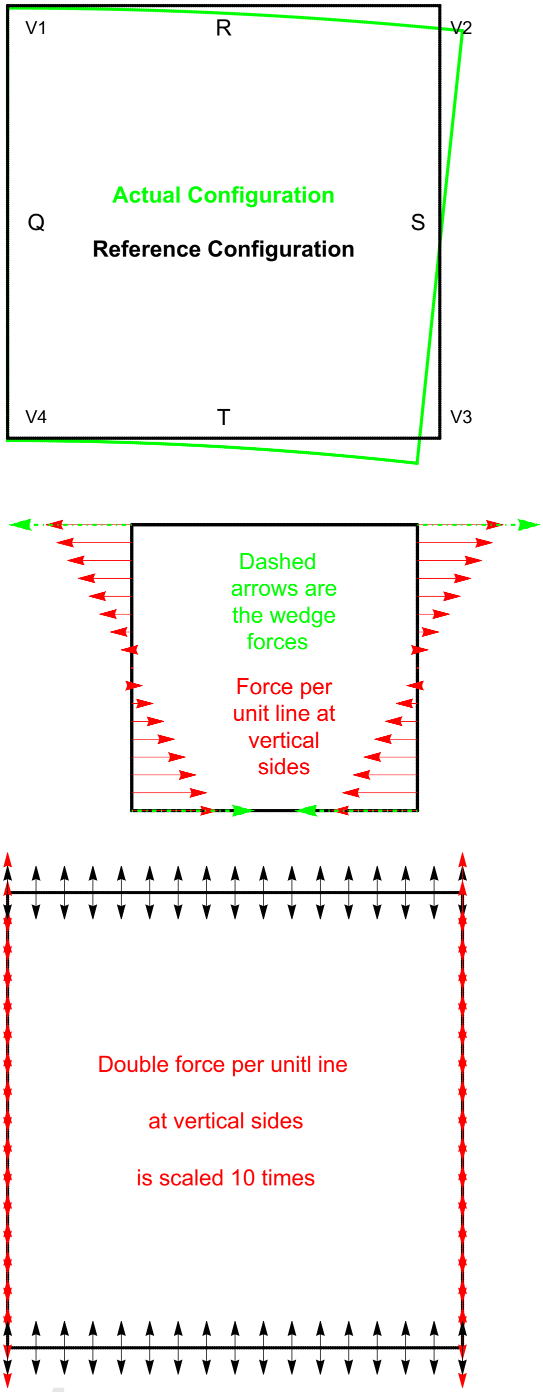

FIG. 5. A *column of figures* is represented for the bent sheet case. In the *first row*, reference and actual configuration are represented. In the *second row*, wedge forces and force per unit line are represented. In the *third row*, we represented the double force per unit line

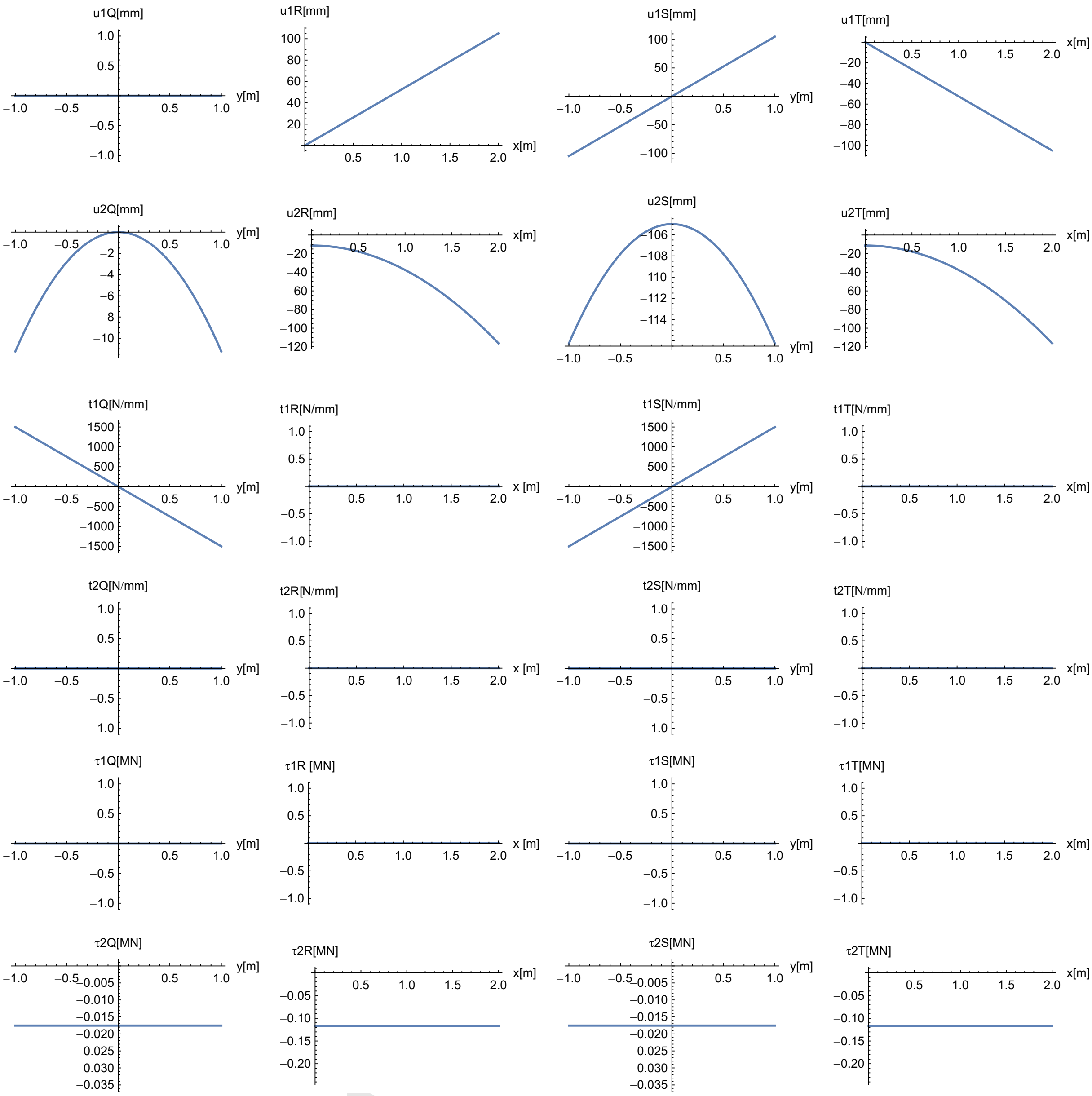

FIG. 6. A *grid of figures* is represented for the bent sheet case. In the *first, second, third* and *fourth column*, we show characteristics of sides A, B, C and D, respectively. In the first and in the *second row*, we show the displacement fields, respectively, in the two directions. In the *third* and in the *fourth row*, we show the force per unit line fields, respectively, in the two directions. In the *fifth* and in the *sixth row*, we show the double force per unit line fields, respectively, in the two directions

In the following, we consider the general solution of this simple problem in the first gradient case. Thus, we calculate the whole set of boundary conditions to be applied in the second gradient case.

3.6.1. The external edge forces. In the following, we calculate the edge forces that are necessary to have the displacement field (69). Such forces per unit line also graphically represented in the second row of Fig. 5 and in the third and fourth rows of Fig. 6.

Side S. From (24) and (69), we have

$$t_1 = t_1^{\text{ext},S} = \frac{3M^{\text{ext}} X_2}{2l^3}. \tag{73}$$

Such force in the horizontal direction is the classical bending solution. We remark that the moment of the force per unit line $t_1^{\text{ext},S}$ is

$$\int_{-l}^{l} t_1^{\text{ext},S} X_2 = \int_{-l}^{l} \frac{3M^{\text{ext}} X_2}{2l^3} X_2 = M^{\text{ext}} \tag{74}$$

that gives a justification of the name of the parameter M^{ext}. We remark that the vertical tip displacement u_t^b of the middle line is from (69)

$$u_t^b = u_2\left(x_1 = L, x_2 = 0\right) = -M^{\text{ext}} \frac{3L^2\left(\lambda + 2\mu\right)}{16l^3 \mu \left(\lambda + \mu\right)},$$

so that

$$M^{\text{ext}} = -u_t^b \frac{16l^3 \mu\left(\lambda + \mu\right)}{3L^2\left(\lambda + 2\mu\right)}. \tag{75}$$

From (25) and (69), we have simply $t_2 = t_2^{\text{ext},S} = 0$.

Side Q. From (28) and (69), we have

$$t_1 = t_1^{\text{ext},Q} = -\frac{3M^{\text{ext}} X_2}{2l^3}, \tag{76}$$

that, for symmetry reasons, is the opposite of that on side S. From (29), we have simply $t_2 = t_2^{\text{ext},Q} = 0$.

Sides R and T. From (32), (33), (36) and (37), we have no traction conditions

$$t_1^{\text{ext},R} = t_2^{\text{ext},R} = t_1^{\text{ext},T} = t_2^{\text{ext},T} = 0, \tag{77}$$

for sides R and T.

3.6.2. The external edge double forces. In the previous subsubsection, we calculated the force per unit line that are necessary to have a solution (69). In this subsubsection, we calculate the analogous double force per unit line. Such double forces per unit line are also graphically represented in the third row of Fig. 5 and in the fifth and sixth rows of Fig. 6.

Side S. From (26) and (69), we simply have $\tau_1 = \tau_1^{\text{ext},S} = 0$, and from (27) and (69), we have

$$\tau_2 = \tau_2^{\text{ext},S} = \frac{3M^{\text{ext}}\left[-\left(5\lambda + 8\mu\right)A + \left(\lambda + 4\mu\right)B + 2\lambda C - \left(4\lambda + 8\mu\right)D\right]}{16l^3 \mu\left(\lambda + \mu\right)}. \tag{78}$$

Side Q. From (30) and (69), we simply have $\tau_1 = \tau_1^{\text{ext},Q} = 0$, and from (31) and (69), we have

$$\tau_2 = \tau_2^{\text{ext},Q} = \tau_2^{\text{ext},S}. \tag{79}$$

Side R. From (34) and (69), we have$\tau_1 = \tau_1^{\text{ext},R} = 0$, and from (35) and (69), we have

$$\tau_2 = \tau_2^{R,ext} = -\frac{3M^{\text{ext}}\left[\left(\lambda + 2\mu\right)A + \left(3\lambda + 2\mu\right)B - \left(2\lambda + 4\mu\right)C - \left(4\lambda + 8\mu\right)D\right]}{16l^3 \mu\left(\lambda + \mu\right)}. \tag{80}$$

Side T. From (38) and (69), we have$\tau_1 = \tau_1^{\text{ext},T} = 0$, and from (33) and (69), we have

$$\tau_2 = \tau_2^{T,ext} = \tau_2^{R,ext}. \tag{81}$$

Journal: 33 Article No.: 588 ☐ TYPESET ☐ DISK ☐ LE ☐ CP Disp.:2015/9/22 Pages: 27

3.6.3. The external wedge forces. We do not impose any kinematical restriction on wedges. This means again that the external (or reaction) wedge forces, in order to have the displacement field (69), are

$$f_{\alpha}^{\text{ext}} = -P_{2\alpha 1} - P_{1\alpha 2}$$

for wedges V_1 and V_3 and the opposite

$$f_{\alpha}^{\text{ext}} = P_{2\alpha 1} + P_{1\alpha 2}$$

for wedges V_2 and V_4. We have from (42) and (69)

$$P_{211} + P_{112} = \frac{3M^{\text{ext}}\left[(\lambda + 2\mu)(A - B + 2C) + 4\mu D\right]}{8l^3\mu(\lambda + \mu)} \cong 0.04\,MN, \tag{82}$$

where the exemplifying numerical values employed are those in (15) and (16), with the assumption $M^{\text{ext}} = 1MNm$. From (43) and (69), on the other hand, we simply have,

$$P_{221} + P_{122} = 0. \tag{83}$$

Thus, the external (or reaction) wedge forces for the four vertices are the following,

$$\left(f_1^{\text{ext}}\right)_{V_1} = -\frac{3M^{\text{ext}}\left[(\lambda + 2\mu)(A - B + 2C) + 4\mu D\right]}{8l^3\mu(\lambda + \mu)} \cong -0.04\,MN, \qquad \left(f_2^{\text{ext}}\right)_{V_1} = 0, \tag{84}$$

$$\left(f_1^{\text{ext}}\right)_{V_2} = \frac{3M^{\text{ext}}\left[(\lambda + 2\mu)(A - B + 2C) + 4\mu D\right]}{8l^3\mu(\lambda + \mu)} \cong 0.04\,MN, \qquad \left(f_2^{\text{ext}}\right)_{V_2} = 0, \tag{85}$$

$$\left(f_1^{\text{ext}}\right)_{V_3} = -\frac{3M^{\text{ext}}\left[(\lambda + 2\mu)(A - B + 2C) + 4\mu D\right]}{8l^3\mu(\lambda + \mu)} \cong -0.04\,MN, \qquad \left(f_2^{\text{ext}}\right)_{V_3} = 0, \tag{86}$$

$$\left(f_1^{\text{ext}}\right)_{V_4} = \frac{3M^{\text{ext}}\left[(\lambda + 2\mu)(A - B + 2C) + 4\mu D\right]}{8l^3\mu(\lambda + \mu)} \cong 0.04\,MN, \qquad \left(f_2^{\text{ext}}\right)_{V_4} = 0, \tag{87}$$

that are also graphically represented in the second row of Fig. 5.

3.7. An analytical solution for flexure

Let us take into account the following displacement field,

$$u_1 = -\frac{QX_2\left[(\lambda + 2\mu)\left(3X_1^2 - X_2^2 - 6LX_1\right) + 2(\lambda + \mu)\left(6l^2 - X_2^2\right)\right]}{16l^3\mu(\lambda + \mu)}, \tag{88}$$

$$u_2 = -\frac{Q\left[(3L - X_1)(\lambda + 2\mu)X_1^2 + 3(L - X_1)\lambda X_2^2\right]}{16l^3\mu(\lambda + \mu)}, \tag{89}$$

also represented in the first row of Fig. 7 and in the first and second rows of Fig. 9. The two partial differential equations (10) and (11) are satisfied with null external force per unit area, $b_1^{\text{ext}} = b_2^{\text{ext}} = 0$, where we have used the following intermediate results,

$$u_{1,1} = \frac{3Q(\lambda + 2\mu)(L - X_1)X_2}{8l^3\mu(\lambda + \mu)}, \quad u_{1,12} = \frac{3Q(\lambda + 2\mu)(L - X_1)}{8l^3\mu(\lambda + \mu)}, \quad u_{2,2} = \frac{3Q\left[(X_1 - L)\lambda X_2\right]}{8l^3\mu(\lambda + \mu)}, \tag{90}$$

$$u_{2,1} = \frac{3Q\left[(X_1 - 2L)X_1(\lambda + 2\mu) + X_2\lambda\right]}{16l^3\mu(\lambda + \mu)}, \quad u_{2,11} = \frac{3Q(\lambda + 2\mu)(X_1 - L)}{8l^3\mu(\lambda + \mu)} = -u_{1,12}, \tag{91}$$

$$u_{1,2} = \frac{3Q\left[(\lambda + 2\mu)\left(X_2^2 - X_1^2 + 2LX_1\right) + 2(\lambda + \mu)\left(X_2^2 - 2l^2\right)\right]}{16l^3\mu(\lambda + \mu)}, \quad u_{2,22} = \frac{3Q\left[(X_1 - L)\lambda\right]}{8l^3\mu(\lambda + \mu)}, \tag{92}$$

In the following, we again consider the general solution of this simple problem in the first gradient case. Thus, we calculate the whole set of boundary conditions in the second gradient case.

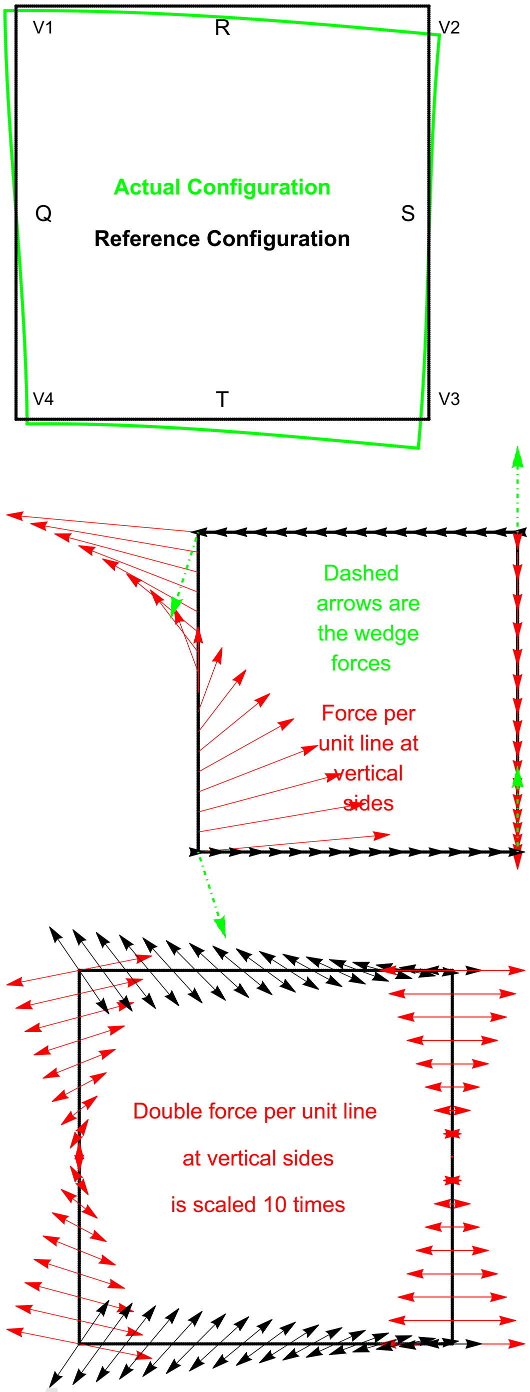

FIG. 7. A *column of figures* is represented for the flexure sheet case. In the *first row*, reference and actual configuration are represented. In the *second row*, wedge forces and force per unit line are represented. In the *third row*, we represented the double force per unit line

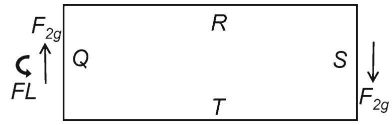

FIG. 8. Graphical scheme for flexure. If the whole set of external force and double force per unit line are not considered, then it is not balanced in the second gradient case

3.7.1. The external edge forces. In the following, we calculate the edge forces that are necessary to have the displacement fields (88) and (89). Such forces per unit line also graphically represented in the second row of Fig. 7 and in the third and fourth rows of Fig. 9.

Side S. From (25) and (88) and (89), we have

$$t_2 = t_2^{\text{ext},S} = -\frac{3F\left[-A\lambda + B\left(5\lambda + 4\mu\right) + 2C\lambda - 4D\left(3\lambda + 4\mu\right) + 4\mu\lambda\left(l^2 - X_2^2\right) + 4\mu^2\left(l^2 - X_2^2\right)\right]}{16l^3\mu\left(\lambda + \mu\right)}. \quad (93)$$

that is the usual force per unit line in the vertical direction and in the first gradient ($A = B = C = D = 0$) and flexural case. We remark that the resultant force, see also the right-hand side of Fig. 8, on the side S is

$$\int_{-l}^{l} t_2^{\text{ext},S} = -F\left[1 + \frac{3\lambda\left(2C - A\right) + 3B\left(5\lambda + 4\mu\right) - 12D\left(3\lambda + 4\mu\right)}{8l^2\mu\left(\lambda + \mu\right)}\right] = -F_{2g} \quad (94)$$

that, on the one hand, it is again equal to $-Q$ in the first gradient ($A = B = C = D = 0$) flexural case. On the other hand, the resultant shear force is equal to $-F_{2g}$ in the present second gradient case. We remark that the downward vertical tip displacement u_t^f of the middle line is from (89)

$$u_t^f = -u_2\left(X_1 = L, X_2 = 0\right) = F\frac{L^3\left(\lambda + 2\mu\right)}{8l^3\mu\left(\lambda + \mu\right)},$$

so that

$$F = u_t^f\frac{8l^3\mu\left(\lambda + \mu\right)}{L^3\left(\lambda + 2\mu\right)}. \quad (95)$$

Besides, the resultant moment on the same side, see again Fig. 8, is null,

$$\int_{-l}^{l} t_1^{\text{ext},S} X_2 = 0. \quad (96)$$

Finally, from (24), (88) and (89) we have simply $t_1 = t_1^{\text{ext},S} = 0$.

Side Q. From (29), we have

$$t_2 = t_2^{\text{ext},Q} = -t_2^{\text{ext},S}, \quad (97)$$

that is the opposite of that on side S, thus giving a vertical resultant

$$\int_{-l}^{l} t_2^{\text{ext},Q} = F_{2g}$$

that is coherent with that shown on the left-hand side of Fig. 8.

From (28), we have simply

$$t_1 = t_1^{\text{ext},Q} = -\frac{3LFX_2}{2l^3}.$$

Such force in the horizontal direction is the usual (in the case $A = B = C = D = 0$) flexural solution as well as its resultant,

$$\int_{-l}^{l} t_1^{\text{ext},Q} = 0,$$

and its moment resultant,

$$\int_{-l}^{l} (-X_2)\, t_1^{\text{ext},Q} = LF,$$

see the left-hand side of Fig. 8.

Sides R and T. From (32), (33), (36) and (37), we have on the one hand no traction conditions in the vertical direction,

$$t_2^{\text{ext},R} = t_2^{\text{ext},T} = 0.$$

On the other hand, in the horizontal direction we need shear force per unit line,

$$t_1^{\text{ext},R} = -t_1^{\text{ext},T} = -\frac{3F}{16l^3\mu\,(\lambda+\mu)}\left[(\lambda+2\mu)\,(A-2C-4D)+B\,(3\lambda+2\mu)\right]. \tag{98}$$

This contradicts the usual no traction condition on the lateral surface on the first gradient case. Thus, (98) means that, in order to have the solution (88) and (89) also in the second gradient case, some shear condition on the lateral surface is necessary.

3.7.2. The external edge double forces. In the previous subsubsection, we calculated the force per unit line that are necessary to have a solution (88) and (89). In this subsubsection, we calculate the analogous double force per unit line. Such double forces per unit line are also graphically represented in the third row of Fig. 7 and in the fifth and sixth rows of Fig. 9.

Side S. From (27), (88) and (89), we simply have $\tau_2 = \tau_2^{\text{ext},C} = 0$ null double force per unit line and from (26), (88) and (89) we have

$$\tau_1 = \tau_1^{\text{ext},S} = \frac{3FX_2\left[(3\lambda+4\mu)\,(A-2C)+\lambda\,(B+4D)\right]}{16l^3\mu\,(\lambda+\mu)}. \tag{99}$$

Side Q. From (31), (88) and (89), we have

$$\tau_2 = \tau_2^{\text{ext},Q} = -\frac{3FL\left[(5\lambda+8\mu)\,A-(\lambda+4\mu)\,B-2\lambda C+(\lambda+2\mu)\,4D\right]}{16l^3\mu\,(\lambda+\mu)}.$$

and from (30), (88) and (89), we have

$$\tau_1 = \tau_1^{\text{ext},Q} = \tau_1^{\text{ext},S}. \tag{100}$$

Side R. From (34), (88) and (89), we have

$$\tau_1 = \tau_1^{\text{ext},R} = \frac{3F\left[(\lambda+2\mu)\,(3A+2C)+(\lambda-2\mu)\,B-4\lambda D\right]}{16l^2\mu\,(\lambda+\mu)}.$$

and from (35), (88) and (89), we have

$$\tau_2 = \tau_2^{R,ext} = -\frac{3F\,(L-X_1)\left[(\lambda+2\mu)\,(A-2C-4D)+(3\lambda+2\mu)\,B\right]}{16l^3\mu\,(\lambda+\mu)}. \tag{101}$$

Side T. From (38), (88) and (89), we have

$$\tau_1 = \tau_1^{\text{ext},T} = -\tau_1^{\text{ext},R}$$

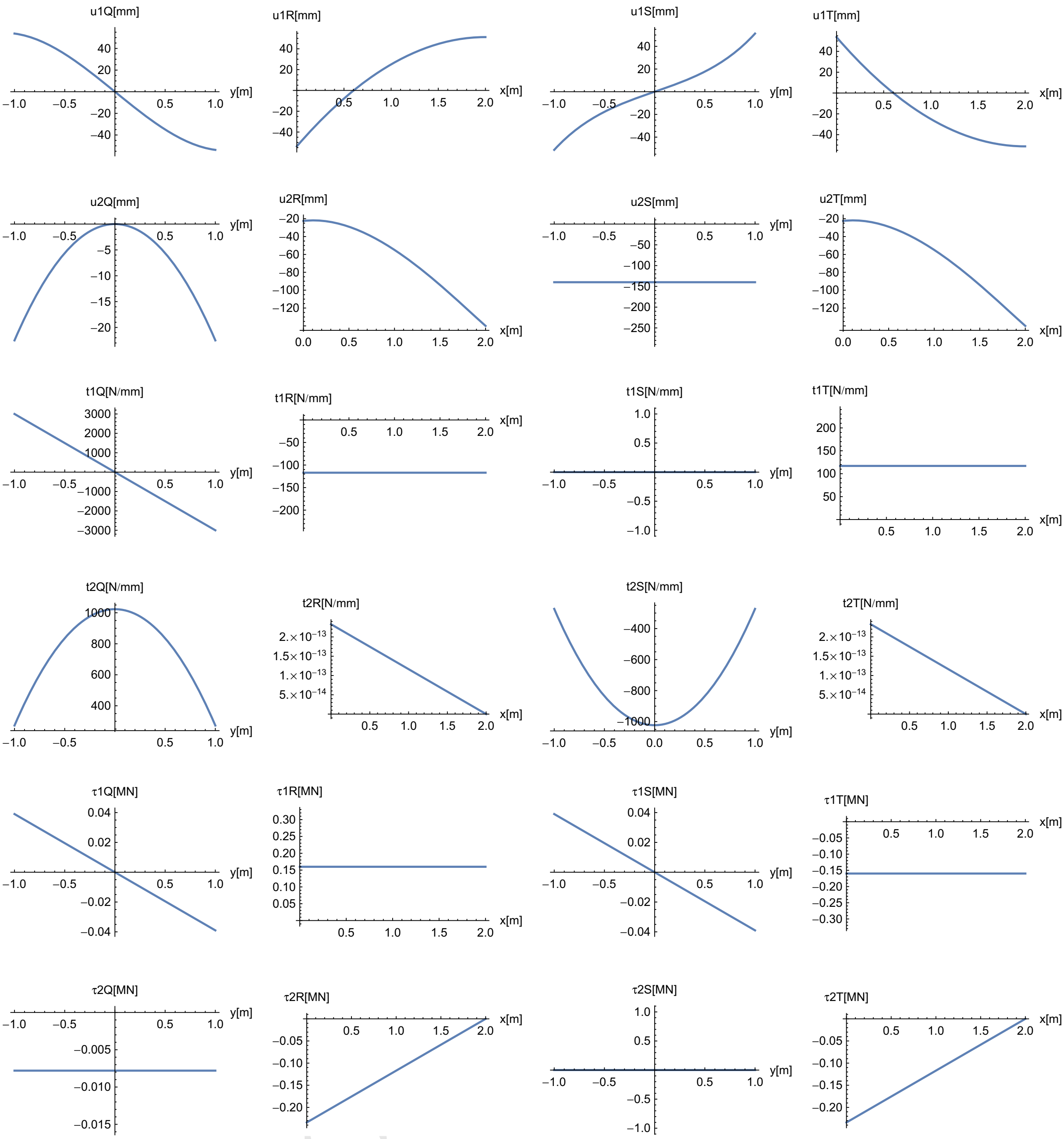

Fig. 9. A *grid of figures* is represented for the flexure sheet case. In the *first, second, third* and *fourth column*, we show characteristics of sides A, B, C and D, respectively. In the *first* and in the *second row*, we show the displacement fields, respectively, in the two directions. In the *third* and in the *fourth row*, we show the force per unit line fields, respectively, in the two directions. In the *fifth* and in the *sixth row*, we show the double force per unit line fields, respectively, in the two directions

and from (33), (88) and (89), we have

$$\tau_2 = \tau_2^{T,ext} = \tau_2^{R,ext}. \tag{102}$$

Journal: 33 Article No.: 588 TYPESET DISK LE CP Disp.:2015/9/22 Pages: 27

3.7.3. The external wedge forces. We do not impose any kinematical restriction on wedges. This means again that the external (or reaction) wedge forces, in order to have the displacement fields (88) and (89), are

$$f_\alpha^{\text{ext}} = -P_{2\alpha 1} - P_{1\alpha 2}$$

for wedges V_1 and V_3 and the opposite

$$f_\alpha^{\text{ext}} = P_{2\alpha 1} + P_{1\alpha 2}$$

for wedges V_2 and V_4. We have from (42), (88) and (89)

$$P_{211} + P_{112} = \frac{3F\left(L - X_1\right)\left[\left(\lambda + 2\mu\right)\left(A - B + 2C\right) + 4\mu D\right]}{8l^3\mu\left(\lambda + \mu\right)},$$

and the numerical values in (15) and (16) are used, for the sake of giving an example, with the assumption $M^{\text{ext}} = 1MN$. From (43), (88) and (89), on the other hand we simply have,

$$P_{221} + P_{122} = -\frac{3Fx_2\left[\left(3\lambda + 4\mu\right)\left(A - B\right) - 2\lambda C + 4\left(2\lambda + 3\mu\right)D\right]}{8l^3\mu\left(\lambda + \mu\right)}.$$

Thus, the external (or reaction) wedge forces for the four vertices are the following,

$$\left(f_1^{\text{ext}}\right)_{V_1} = -\frac{3QL\left[\left(\lambda + 2\mu\right)\left(A - B + 2C\right) + 4\mu D\right]}{8l^3\mu\left(\lambda + \mu\right)} \cong -0.085\,MN, \tag{103}$$

$$\left(f_2^{\text{ext}}\right)_{V_1} = \frac{3Q\left[\left(3\lambda + 4\mu\right)\left(A - B\right) - 2\lambda C + 4\left(2\lambda + 3\mu\right)D\right]}{8l^2\mu\left(\lambda + \mu\right)} \cong -0.27\,MN, \tag{104}$$

$$\left(f_1^{\text{ext}}\right)_{V_2} = 0, \quad \left(f_2^{\text{ext}}\right)_{V_2} = -\frac{3Q\left[\left(3\lambda + 4\mu\right)\left(A - B\right) - 2\lambda C + 4\left(2\lambda + 3\mu\right)D\right]}{8l^2\mu\left(\lambda + \mu\right)} \cong 0.27\,MN, \tag{105}$$

$$\left(f_1^{\text{ext}}\right)_{V_3} = 0, \quad \left(f_2^{\text{ext}}\right)_{V_3} = -\frac{3Q\left[\left(3\lambda + 4\mu\right)\left(A - B\right) - 2\lambda C + 4\left(2\lambda + 3\mu\right)D\right]}{8l^2\mu\left(\lambda + \mu\right)} \cong 0.27\,MN, \tag{106}$$

$$\left(f_1^{\text{ext}}\right)_{V_4} = \frac{3QL\left[\left(\lambda + 2\mu\right)\left(A - B + 2C\right) + 4\mu D\right]}{8l^3\mu\left(\lambda + \mu\right)} \cong 0.085\,MN, \tag{107}$$

$$\left(f_2^{\text{ext}}\right)_{V_4} = \frac{3Q\left[\left(3\lambda + 4\mu\right)\left(A - B\right) - 2\lambda C + 4\left(2\lambda + 3\mu\right)D\right]}{8l^2\mu\left(\lambda + \mu\right)} \cong -0.27\,MN, \tag{108}$$

that are also graphically represented in the second row of Fig. 7.

4. An important conclusion from these analytical solutions

In this section, we prove that if we are able to produce the simple displacement fields (45) in the presence of gravity for the heavy sheet, the simple displacement field (69) for bending and the simple displacement fields (88) and (89) for flexure, then we can measure the 4 independent constitutive coefficients A, B, C and D by just measuring forces.

For the heavy sheet, we measure the maximum lateral forces R_1^{hs} from (48) or (49) at the top of vertical sides due to Poisson effects,

$$R_1^{hs} = t_1^{\text{ext},S}\left(x_2 = l\right) = \frac{2\lambda l\rho g}{\left(\lambda + 2\mu\right)}, \tag{109}$$

the vertical displacement at the bottom-side T from (69)

$$R_2^{hs} = u_2\left(x_1, x_2 = -l\right) = -\frac{2l^2\rho g}{\left(\lambda + 2\mu\right)}, \tag{110}$$

Journal: 33 Article No.: 588 TYPESET DISK LE CP Disp.:2015/9/22 Pages: 27

the necessary horizontal wedge forces (56) at vertices of the rectangular sheet,

$$R_3^{hs} = \frac{2D\rho g}{(\lambda + 2\mu)}, \tag{111}$$

and the necessary vertical forces from (68) at vertices of the trapezoidal sheet,

$$R_4^{hs} = \sin\theta\cos\theta\left[\frac{\rho g}{2(\lambda + 2\mu)}(B - A + 2C)\right]. \tag{112}$$

For the bending case, we measure the necessary horizontal wedge forces from (82) in one of the 4 vertices,

$$R_5^b = \left(f_1^{\text{ext}}\right)_{V_2} = \frac{3M^{\text{ext}}\left[(\lambda + 2\mu)(A - B + 2C) + 4\mu D\right]}{8l^3\mu(\lambda + \mu)}, \tag{113}$$

where the resultant bending force M^{ext} is given by (75) and it is not independent of that of (109) and of (111).

For the flexural case, we measure (i) the maximum vertical force per unit line at side S at the middle point $x_2 = 0$,

$$R_6^f = t_2^{\text{ext},S}(x_1 = L, x_2 = 0) = \frac{3F\left[-A\lambda + B(5\lambda + 4\mu) + 2C\lambda - 4D(3\lambda + 4\mu) + 4\mu l^2(\lambda + \mu)\right]}{16l^3\mu(\lambda + \mu)}, \tag{114}$$

where the parameter F is related to the resultant bending force via the (94) and to the vertical tip displacement via the (95); (ii) the horizontal shear force on sides R or T from (98),

$$R_7^f = t_1^{\text{ext},T} = \frac{3F}{16l^3\mu(\lambda + \mu)}\left[(\lambda + 2\mu)(A - 2C - 4D) + B(3\lambda + 2\mu)\right]; \tag{115}$$

(iii) the horizontal wedge force at one of the left-hand side wedges,

$$R_8^f = \left(f_1^{\text{ext}}\right)_{V_4} = \frac{3FL\left[(\lambda + 2\mu)(A - B + 2C) + 4\mu D\right]}{8l^3\mu(\lambda + \mu)}, \tag{116}$$

and (iv) one of the vertical wedge forces at one of the 4 vertices,

$$R_9^f = \left(f_2^{\text{ext}}\right)_{V_4} = \frac{3F\left[(3\lambda + 4\mu)(A - B) - 2\lambda C + 4(2\lambda + 3\mu)D\right]}{8l^2\mu(\lambda + \mu)}. \tag{117}$$

On the one hand, Gedanken experiments (109) and (110) can be used to evaluate the Lamé coefficients λ and μ. Gedanken experiments (111), (112), (113) and (114) are, on the other hand, sufficient to measure the 4 independent coefficients A, B, C and D. The results in (115), (116) and (117) can also be used.

5. Conclusion

A two-dimensional solid consisting of a linear elastic isotropic material has been considered, where the strain energy, within the framework of objectivity and isotropy, has been expressed as the most general function of the strain and of the gradient of strain. Variational methods have been used to formulate the corresponding balance equations and boundary conditions. In this paper, analytical solutions of this problem have been outlined with the purpose of identifying the whole set of constitutive parameters. This has been achieved through the design of some ideal experiments that allow to write equations that having as unknowns such a set of constants and as known terms the values of the experimental measurements. The results of this work can provide a theoretical and practical guide to the design of laboratory experiments, capable of identifying all the constitutive parameters of the $2D$ solids, characterized by strain energy density dependent on the first and second gradient of the displacement.

References

1. Alibert, J., Seppecher, P., dell'Isola, F.: Truss modular beams with deformation energy depending on higher displacement gradients. Math. Mech. Solids **8**(1), 51–73 (2003)
2. Altenbach, H., Eremeev, V.A., Morozov, N.F.: On equations of the linear theory of shells with surface stresses taken into account. Mech. Solids **45**(3), 331–342 (2010)
3. Auffray, N.: On the isotropic moduli of 2D strain-gradient elasticity. Contin. Mech. Thermodyn. **27**(1–2), 5–19 (2015)
4. Bersani, A.M., Giorgio, I., Tomassetti, G.: Buckling of an elastic hemispherical shell with an obstacle. Contin. Mech. Thermodyn. **25**(2–4), 443–467 (2013)
5. Bilotta, A., Turco, E.: A numerical study on the solution of the Cauchy problem in elasticity. Int. J. Solids Struct. **46**(25–26), 4451–4477 (2009)
6. Carassale, L., Freda, A., Marrè-Brunenghi, M.: Effects of free-stream turbulence and corner shape on the galloping instability of square cylinders. J. Wind Eng. Ind. Aerodyn. **123**, 274–280 (2013)
7. Cazzani, A., Ruge, P.: Numerical aspects of coupling strongly frequency-dependent soil-foundation models with structural finite elements in the time-domain. Soil Dyn. Earthq. Eng. **37**, 56–72 (2012)
8. Cesarano, C., Assante, D.: A note on generalized Bessel functions. Int. J. Math. Models Methods Appl. Sci. **8**(1), 38–42 (2014)
9. Cuomo, M., Contrafatto, L., Greco, L.: A variational model based on isogeometric interpolation for the analysis of cracked bodies. Int. J. Eng. Sci. **80**, 173–188 (2014)
10. de Oliveira Góes, R.C., de Castro, J.T.P., Martha, L.F.: 3D effects around notch and crack tips. Int. J. Fatigue **62**, 159–170 (2014)
11. Dos Reis, F., Ganghoffer, J.F.: Construction of micropolar continua from the asymptotic homogenization of beam lattices. Comput. Struct. **112–113**, 354–363 (2012)
12. Del Vescovo, D., Giorgio, I.: Dynamic problems for metamaterials: review of existing models and ideas for further research. Int. J. Eng. Sci. **80**, 153–172 (2014)
13. dell'Isola, F., Andreaus, U., Placidi, L.: At the origins and in the vanguard of peri-dynamics, non-local and higher gradient continuum mechanics. An underestimated and still topical contribution of Gabrio Piola. Mech. Math. Solids (2014). doi:10.1177/1081286513509811 update as follows: vol. 20, p. 887-928, year 2015, ISSN 1081-2865
14. dell'Isola, F., Gouin, H., Seppecher, P.: Radius and surface tension of microscopic bubbles by second gradient theory. C. R. Acad. Sci. Ser. **320**(6), 211–216 (1995)
15. dell'Isola, F., Gouin, H., Rotoli, G.: Nucleation of spherical shell-like interfaces by second gradient theory: Numerical simulations. Eur. J. Mech. B/Fluids **15**(4), 545–568 (1996)
16. dell'Isola, F., Guarascio, M., Hutter, K.: A variational approach for the deformation of a saturated porous solid. A second-gradient theory extending Terzaghi's effective stress principle. Arch. Appl. Mech. **70**(5), 323–337 (2000)
17. dell'Isola, F., Madeo, A., Placidi, L.: Linear plane wave propagation and normal transmission and reflection at discontinuity surfaces in second gradient 3D Continua. Z. Angew. Math. Mech. **92**(1), 52–71 (2012)
18. dell'Isola, F., Madeo, A., Seppecher, P.: Boundary conditions at fluid-permeable interfaces in porous media: a variational approach. Int. J. Solids Struct. **46**(17), 3150–3164 (2009)
19. dell'Isola, F., Rotoli, G.: Validity of Laplace formula and dependence of surface tension on curvature in second gradient fluids. Mech. Res. Commun. **22**(5), 485–490 (1995)
20. dell'Isola, F., Sciarra, G., Batra, R.: A second gradient model for deformable porous matrices filled with an inviscid fluid. In: IUTAM Symposium on Physicochemical and Electromechanical Interactions in Porous Media. Solid Mechanics and its Applications, vol. 125, pp. 221–229 (2005)
21. dell'Isola, F., Sciarra, G., Batra, R.: Static deformations of a linear elastic porous body filled with an inviscid fluid. J. Elast. **72**(1–2), 99–120 (2003)
22. dell'Isola, F., Sciarra, G., Vidoli, S.: Generalized Hooke's law for isotropic second gradient materials. R. Soc. Lond. **465**(107), 2177–2196 (2009)
23. dell'Isola, F., Seppecher, P.: Commentary about the paper hypertractions and hyperstresses convey the same mechanical information. Contin. Mech. Thermodyn. **22**, 163–176 (2010) by Prof. Podio Guidugli and Prof. Vianello and some related papers on higher gradient theories. Contin. Mech. Thermodyn. **23**(5), 473–478 (2011): R. Soc. Lond. ,
24. dell'Isola, F., Seppecher, P.: Edge contact forces and quasi-balanced power. Meccanica **32**(1), 33–52 (1997)
25. dell'Isola, F., Seppecher, P.: The relationship between edge contact forces, double forces and interstitial working allowed by the principle of virtual power. C. R. Acad. Sci. Ser. **321**, 303–308 (1995)
26. dell'Isola, F., Steigmann, D.: A two-dimensional gradient-elasticity theory for woven fabrics. J. Elast. **118**(1), 113–125 (2015)
27. Federico, S.: On the linear elasticity of porous materials. Int. J. Mech. Sci. **52**, 175–182 (2010)
28. Federico, S.: Covariant formulation of the tensor algebra of non-linear elasticity. Int. J. Nonlinear Mech. **47**, 273–284 (2012)

29. Federico, S.: Volumetric-distortional decomposition of deformation and elasticity tensor. Math. Mech. Solids **15**, 672–690 (2010)
30. Federico, S., Grillo, A., Herzog, W.: A transversely isotropic composite with a statistical distribution of spheroidal inclusions: a geometrical approach to overall properties. J. Mech. Phys. Solids **52**, 2309–2327 (2004)
31. Federico, S., Grillo, A., Imatani, S.: The linear elasticity tensor of incompressible materials. Math. Mech. Solids (2014). doi:10.1177/1081286514550576 update as follows: vol. 20, 6: pp. 643-662, year 2015, ISSN: 1081-2865
32. Federico, S., Grillo, A., Wittum, G.: Considerations on incompressibility in linear elasticity. Nuovo Cimento C **32**, 81–87 (2009)
33. Ferretti, M., Madeo, A., dell'Isola, F., Boisse, P.: Modelling the onset of shear boundary layers in fibrous composite reinforcements by second gradient theory. Z. Angew. Math. Phys. **65**(3), 587–612 (2014)
34. Goda, I., Assidi, M., Ganghoffer, J.F.: A 3D elastic micropolar model of vertebral trabecular bone from lattice homogenization of the bone microstructure. Biomech. Model. Mechanobiol. **13**(1), 53–83 (2014)
35. Goda, I., Rahouadj, R., Ganghoffer, J.-F.: Size dependent static and dynamic behavior of trabecular bone based on micromechanical models of the trabecular architecture. Int. J. Eng. Sci. **72**, 53–77 (2013)
36. Goda, I., Assidi, M., Belouettar, S., Ganghoffer, J.F.: A micropolar anisotropic constitutive model of cancellous bone from discrete homogenization. J. Mech. Behav. Biomed. Mater. **16**(1), 87–108 (2012)
37. Garusi, E., Tralli, A., Cazzani, A.: An unsymmetric stress formulation for Reissner-Mindlin plates: a simple and locking-free rectangular element. Int. J. Comput. Eng. Sci. **5**(3), 589–618 (2004)
38. Greco, L., Cuomo, M.: Consistent tangent operator for an exact Kirchhoff rod model. Contin. Mech. Thermodyn. **27**(4), 861–877 (2015)
39. Hill, R.: A self-consistent mechanics of composite materials. J. Mech. Phys. Solids **13**, 213–222 (1965)
40. Madeo, A., dell'Isola, F., Darve, F.: A continuum model for deformable, second gradient porous media partially saturated with compressible fluids. J. Mech. Phys. Solids **61**(11), 2196–2211 (2013)
41. Madeo, A., dell'Isola, F., Ianiro, N., Sciarra, G.: A variational deduction of second gradient poroelasticity II: An application to the consolidation problem. J. Mech. Mater. Struct. **3**(4), 607–625 (2008)
42. Madeo, A., Neff, P., Ghiba, I.-D., Placidi, L., Rosi, G.: Band gaps in the relaxed linear micromorphic continuum. Z. Angew. Math. Mech. ISSN:1521-4001. doi:10.1002/zamm.201400036 update as follows: Volume 95, Issue 9, pages 880–887, year 2015
43. Mindlin, R.D.: Micro-structure in Linear Elasticity. Department of Civil Engineering, Columbia University, New York (1964)
44. Misra, A., Singh, V.: Nonlinear granular micromechanics model for multi-axial rate-dependent behavior. Int. J. Solids Struct. **51**(13), 2272–2282 (2014)
45. Misra, A., Parthasarathy, R., Singh, V., Spencer, P.: Micro-poromechanics model of fluid-saturated chemically active fibrous media. Z. Angew. Math. Mech. **95**(2), 215–234 (2015)
46. Neff, P., Ghiba, I.-D., Madeo, A., Placidi, L., Rosi, G.: A unifying perspective: the relaxed linear micromorphic continuum. Contin. Mech. Thermodyn. **26**(5), 639–681 (2014). ISSN:0935-1175. doi:10.1007/s00161-013-0322-9
47. Neff, P., Jeong, J., Ramézani, H.: Subgrid interaction and micro-randomness—novel invariance requirements in infinitesimal gradient elasticity. Int. J. Solids Struct. **46**(25), 4261–4276 (2009)
48. Nguyen, C.H., Freda, A., Solari, G., Tubino, F.: Aeroelastic instability and wind-excited response of complex lighting poles and antenna masts. Eng. Struct. **85**, 264–276 (2015)
49. Pagnini, L.: Reliability analysis of wind-excited structures. J. Wind Eng. Ind. Aerodyn. **98**(1), 1–9 (2010)
50. Pagnini, L.C., Solari, G.: Serviceability criteria for wind-induced acceleration and damping uncertainties. J. Wind Eng. Ind. Aerodyn. **74–76**, 1067–1078 (1998)
51. Pagnini, L.C.: Model reliability and propagation of frequency and damping uncertainties in the dynamic along-wind response of structures. J. Wind Eng. Ind. Aerodyn. **59**(2–3), 211–231 (1996)
52. Piccardo, G., Ranzi, G., Luongo, A.: A complete dynamic approach to the Generalized Beam Theory cross-section analysis including extension and shear modes. Math. Mech. Solids **19**(8), 900–924 (2014)
53. Placidi, L.: A variational approach for a nonlinear one-dimensional damage-elasto-plastic second-gradient continuum model. Contin. Mech. Thermodyn. ISSN:0935-1175. doi:10.1007/s00161-014-0405-2
54. Placidi, L.: A variational approach for a nonlinear 1-dimensional second gradient continuum damage model. Contin. Mech. Thermodyn. **27**(4), 623–638 (2015). ISSN:0935-1175. doi:10.1007/s00161-14-0338-9
55. Placidi, L., El Dhaba, A.R.: Semi-inverse method la Saint-Venant for two-dimensional linear isotropic homogeneous second gradient elasticity. Mech. Math. Solids (accepted). ISSN:1081-2865
56. Rinaldi, A., Placidi, L.: A microscale second gradient approximation of the damage parameter of quasi-brittle heterogeneous lattices. Z. Angew. Math. Mech. **94**, 862–877 (2015)
57. Rosi, G., Giorgio, I., Eremeyev, V.A.: Propagation of linear compression waves through plane interfacial layers and mass adsorption in second gradient fluids. Z. Angew. Math. Mech. **93**(12), 914–927 (2013)
58. Roveri, N., Carcaterra, A., Akay, A.: Vibration absorption using non-dissipative complex attachments with impacts and parametric stiffness. J. Acoust. Soc. Am. **126**(5), 2306–2314 (2009)

59. Sansour, C., Skatulla, S.: A strain gradient generalized continuum approach for modelling elastic scale effects. Comput. Methods Appl. Mech. Eng. **198**(15), 1401–1412 (2009)
60. Sciarra, G., dell'Isola, F., Coussy, O.: Second gradient poromechanics. Int. J. Solids Struct. **44**(20), 6607–6629 (2007)
61. Sciarra, G., dell'Isola, F., Ianiro, N., Madeo, A.: A variational deduction of second gradient poroelasticity part I: general theory. J. Mech. Mater. Struct. **3**(3), 507–526 (2008)
62. Selvadurai, A.P.S.: Plane strain problems in second-order elasticity theory. Int. J. Nonlinear Mech. **8**(6), 551–563 (1973)
63. Selvadurai, A.P.S., Spencer, A.J.M.: Second-order elasticity with axial symmetry-I. General theory. Int. J. Eng. Sci. **10**(2), 97–114 (1972)
64. Seppecher, P., Alibert, J.-J., dell'Isola, F.: Linear elastic trusses leading to continua with exotic mechanical interactions. J. Phys. Conf. Ser. **319**(1), 13 (2011)
65. Solari, G., Pagnini, L.C., Piccardo, G.: A numerical algorithm for the aerodynamic identification of structures. J. Wind Eng. Ind. Aerodyn. **69–71**, 719–730 (1997)
66. Steigmann, D.J.: Linear theory for the bending and extension of a thin, residually stressed, fiber-reinforced lamina. Int. J. Eng. Sci. **47**(11–12), 1367–1378 (2009)
67. Steigmann, D.J., dell'Isola, F.: Mechanical response of fabric sheets to three-dimensional bending, twisting, and stretching. Acta Mech. Sin./Lixue Xuebao **31**(3), 373–382 (2015)
68. Terravecchia, S., Panzeca, T., Polizzotto, C.: Strain gradient elasticity within the symmetric BEM formulation. Fract. Struct. Integr. **29**, 61–73 (2014)
69. Turco, E.: Identification of axial forces on statically indeterminate pin-jointed trusses by a nondestructive mechanical test. Open Civ. Eng. J. **7**(1), 50–57 (2013)
70. Walpole, L.J.: Elastic behavior of composite materials: theoretical foundations. Adv. Mech. **21**, 169–242 (1981)
71. Walpole, L.J.: Fourth-rank tensors of the thirty-two crystal classes: multiplication tables. Proc. R. Soc. Lond. Ser. A **391**, 149–179 (1984)
72. Yang, Y., Misra, A.: Micromechanics based second gradient continuum theory for shear band modeling in cohesive granular materials following damage elasticity. Int. J. Solids Struct. **49**(18), 2500–2514 (2012)

Luca Placidi
International Telematic University Uninettuno
C. so Vittorio Emanuele II,
39 00186 Rome
Italy
e-mail: luca.placidi@uninettunouniversity.net

Ugo Andreaus and Alessandro Della Corte
Universitá di Roma La Sapienza
Rome
Italy

Tomasz Lekszycki
Faculty of Engineering Production
Warsaw University of Technology
Warsaw
Poland

(Received: March 31, 2015; revised: September 7, 2015)

Journal: 33 Article No.: 588 ☐ TYPESET ☐ DISK ☐ LE ☐ CP Disp.:2015/9/22 Pages: 27